Evolutionary Ecology Research, 2010, **12**: 897–928

Functional and phylogenetic constraints in Rhinocerotinae craniodental morphology

Paolo Piras[1], Leonardo Maiorino[1], Pasquale Raia[1,2], Federica Marcolini[1], Daniele Salvi[1,4], Leonardo Vignoli[1,3] and Tassos Kotsakis[1,5]

[1]*Center for Evolutionary Ecology, Università di Roma Tre, Rome, Italy,*
[2]*Earth Science Department, Università di Napoli Federico II, Naples, Italy,*
[3]*Department of Environmental Biology, Università di Roma Tre, Rome, Italy,*
[4]*CIBIO, Centro de Investigação em Biodiversidade e Recursos Genéticos, Campus Agrário de Vairão, Vairão, Portugal and* [5]*Geological Sciences Department, Università di Roma Tre, Rome, Italy*

ABSTRACT

Hypotheses: After the effect of phylogeny is statistically removed, cranial structures that are employed solely for mastication should covary the most with hypsodonty (high-crowned cheek teeth are termed 'hypsodont'). Such structures should also be the least phylogenetically constrained. A corollary: structures that are highly influenced by shared ancestry will exhibit greater morphological integration than those that are affected less.

Organisms: All extant rhinoceroses and a number of extinct, European, Plio-Pleistocene species.

Analytical methods: Using two-dimensional geometric morphometrics, we studied skull shape in the dorsal and lateral views, mandible shape in the lateral view, and the upper tooth row shape in the occlusal view. To reflect feeding habits, we used a surrogate variable, the hypsodonty index. Using phylogenetically independent contrasts and variation partitioning, we separated shape variation into function, phylogeny, and size components. We tested morphological integration with Escoufier's *RV* coefficient.

Results: The mandible and the upper tooth row have the highest covariance with hypsodonty and the least with phylogeny. Skull morphology shows the reverse; it has the smallest covariance with hypsodonty and the highest with phylogeny. The degree of morphological integration between the upper tooth row and the other structures is relatively low, indicating that the former component is the least phylogenetically constrained. In keeping with our predictions, the cranial region associated with chewing is constrained by function and not as much by phylogeny, whereas others show stronger phylogenetic constraint.

Keywords: comparative methods, craniodental morphology, Europe, feeding habits, geometric morphometrics, Plio-Pleistocene, Rhinocerotinae.

Correspondence: P. Piras, Geological Science Department and Center for Evolutionary Ecology, Largo S. Leonardo Murialdo 1, 00146 Rome, Italy. e-mail: ppiras@uniroma3.it

INTRODUCTION

Ungulate diets and the environments they live in are closely connected (Sponheimer *et al.*, 2003). Dietary preferences in these mammals correlate with morphological specialization in both digestive strategy (Janis, 1976; Demment and Van Soest, 1985; Clauss *et al.*, 2003; Clauss and Hummel, 2005) and skull morphology, affecting rostrum, mandible, and tooth shapes (Gordon and Illius, 1988; Solounias *et al.*, 1988, 1995; Janis, 1995; Perez-Barberia and Gordon, 1999, 2001; Williams and Kay, 2001; Mendoza *et al.*, 2002; Mendoza and Palmqvist, 2008; Raia *et al.*, 2010).

This close association between diet and morphology allows feeding habits in extinct species to be inferred. Even when no intelligible cranial remains are available, diets can still be ascertained with some accuracy by calculating the relative molar teeth crown height (the so-called hypsondonty index). In fact, short-crowned molars usually indicate a diet of soft plants (i.e. browsing), whereas high-crowned molars indicate grass feeding (i.e. grazing).

However, Fortelius and Solounias (2000) suggested that hypsodonty belongs to the preformed adaptations in deep time and for this reason it might, occasionally, be a poor indicator of diet. They proposed the method of 'mesowear' as a tool to allow finer inference of diet in extinct and extant species. Using this method, Kahlke and Kaiser (in press) found that *Stephanorhinus hundsheimensis*, a very common rhino in the Early and Middle Pleistocene of Europe, had very different dietary preferences at two different German sites, reflecting an overall catholic diet enabling the species to adapt to different food types. Mesowear analysis measures the abrasiveness of different diets on cheek teeth by inspection of the development of tooth facets and cusp shape (Fortelius and Solounias, 2000). Fortelius and Solounias (2000) argued that hypsodonty is essentially a reflection of the overall tooth wear rate, and its relationship with food quality is expected to be considerably less specific than that with mesowear. In contrast, when large-scale dietary classes are used, short-crowned molars consistently indicate a browsing diet, whereas high-crowned molars allow feeding on grasses, or grazing (Feranec, 2007).

Although variation in craniodental shape is correlated with diet, several recent studies argue against the idea that this correlation is promoted by adaptation (Pérez-Barberia and Gordon, 1999, 2001; Raia *et al.*, 2010). Pérez-Barberia and Gordon (1999, 2001) tested the correlation of several morphological cranial variables with diet in ungulates, and found that only the length of the coronoid process, body size, and hypsodonty index correlate well with feeding habits after phylogeny is accounted for. Raia *et al.* (2010) found that ungulate mandible shape is significantly affected by hypsodonty index, but only above the species level, and in combination with the differences in digestive anatomy between odd- and even-toed species. The relationship between diet and craniodental variation in herbivore crania is very complex because of the functional, phylogenetic, and biomechanical constraints in design that affect such a multi-purpose structure (Meloro *et al.*, 2008; Raia *et al.*, 2010), and which need to be integrated with each other to some extent to allow for optimal performance of their common function (Klingenberg, 2009), which is mastication. Rhinos are interesting in this regard because of their peculiar skull morphology, their long evolutionary history, and the variety of feeding adaptations they acquired in the past, and in part show nowadays.

Rhinos first appeared in North America, Europe, and Asia with the genus *Hyrachyus* in the middle Eocene, and have diversified since in a great variety of forms spread over all continents except South America and Oceania. Most authors currently accept that there are three valid families of rhinos – Hyracodontidae, Amynodontidae, and Rhinocerotidae – whose diversity (taken as a whole) swung dramatically from a peak during the Miocene

to the current paucity of species. Extant rhinos (all belonging to Rhinocerotidae) are represented by only four genera and five species (*Ceratotherium simum*, *Diceros bicornis*, *Rhinoceros unicornis*, *Rhinoceros sondaicus*, and *Dicerorhinus sumatrensis*).

Zeuner (1934) first highlighted that browsing and grazing rhinos possess different angles between the occiput and the palate due to different head posture during feeding. Bales (1996) analysed the morphological variation in extant rhinos' skulls in relation to the orientation of the masseter and posterior temporalis muscles. He then extended his comparisons to the early Oligocene genus *Subhyracodon*, which he deemed to be 'representative of the primitive rhinoceros skull condition', by means of two-dimensional geometric morphometrics. Bales (1996) concluded that mandibular suspension evolved according to the feeding habits in the extant rhino skulls and to the head posture during feeding in an adaptive fashion. However, he recognized that both adaptation and phylogenetic inheritance had played a role in moulding skull shape variation during rhinos' history, but without providing any quantitative assessment for this notion.

Exploring the interplay between morphology, function, and phylogeny pertains to the debate about the nature of 'constraints' in the evolutionary process. The meaning of the term 'constraint' has led to many disputes. Schwenk (1995) argued that phylogeny cannot be considered a constraint in itself because it is just the result (i.e. a pattern) of historical contingency. Maynard Smith *et al.* (1985), Gould and Lewontin (1979), Arthur (2001), and Gould (2002) suggested a positive meaning of the term 'constraint' for it might promote new heritable variation. Independently of the preferred semantics used indicating the role of phylogenetic inheritance and adaptation in evolution, these two aspects should be considered simultaneously when the phenotype (i.e. morphology in this study) is under investigation. As for the meaning of 'adaptation' with reference to biological structures, we adopt a narrow definition, which is any heritable trait that signifies a solution to a problem that current environmental conditions present and that appears simultaneously or soon after the new environmental condition sets in (after Arnold, 1994; Strömberg, 2006; cf. Gould and Vrba, 1982). In the present context, such an adaptation is the evolution of high-crowned molars, as measured by relative molar crown height or the 'hypsodonty index'.

We investigated the influence of phylogeny, size, and hypsodonty index on Rhinocerotinae craniodental morphology by means of two different comparative methods, phylogenetically independent contrasts and variation partitioning. The hypsodonty index is not presumed to be equally associated with morphological changes in different craniodental anatomical regions.

We assessed the degree of morphological integration among three hypothesized craniodental modules (skull – captured in the dorsal and lateral views – mandible, and upper tooth row). Although the skull region simplifies a complex system that previous studies have demonstrated actually encompasses multiple phenotypic modules (e.g. Cheverud, 1982, 1989, 1995; Zelditch, 1988; Zelditch and Carmichael, 1989a, 1989b; Leamy *et al.*, 1999; Ackermann and Cheverud, 2000, 2004a, 2004b; Lieberman *et al.*, 2000; Marroig and Cheverud, 2001; Strait, 2001; Hallgrímsson *et al.*, 2002; Marroig *et al.*, 2004; Zelditch and Moscarella, 2004; Bastir and Rosas, 2005, 2006; Goswami, 2006; Goswami and Prochel, 2007; Drake and Klingenberg, 2010; Goswami and Polly, 2010; Piras *et al.*, 2010), the point here is to distinguish the regions most involved in mastication (mandible and upper tooth row) from the rest of the cranium. While several studies have examined morphological integration within the mammalian mandible (Atchley *et al.*, 1982; Atchley and Hall, 1991; Cheverud *et al.*, 1991, 1997, 2004; Atchley, 1993; Badyaev and Foresman, 2000, 2004; Klingenberg and Leamy, 2001; Klingenberg *et al.*, 2001, 2003, 2004; Leamy *et al.*, 2002; Ehrich *et al.*, 2003; Cheverud, 2004; Badyaev *et al.*, 2005; Polly, 2005; Márquez, 2008; Klingenberg, 2009; Zelditch *et al.*, 2009), relatively

few have directly compared the integration of the mandible with other cranial regions. Our specific aim here is to interpret the morphological integration between these structures as a constraint on their morphological variation. This allows us to test the prediction that morphological integration between parts should be lowest where the influence of adaptation is the greatest. This is the case because strong integration among modules may act as a constraint (Klingenberg, 2005; Drake and Klingenberg, 2010; Goswami and Polly, 2010), and patterns of morphological integration are expected to reflect functional association among parts (Wagner and Altenberg, 1996). In the present context, we predict that the mandible and the upper tooth row will show greater covariation with the hypsodonty index than with the skull. Usually, modularity studies have the aim of testing the reliability of modules *a posteriori* starting from *a priori* hypotheses about modular structure *within* super-modules [e.g. the vertebrate mandible (Márquez, 2008) or *Drosophila* wings (Klingenberg, 2009)]. There is no reason here to test *a posteriori* our modular hypothesis, as these structures are physically independent (tooth row, mandibles, and skull). Moreover, we want here to measure the *covariation between* the four configurations, rather than to explore their inner modularity patterns.

Young and Hallgrímsson (2005) investigated the covariation structure between forelimb and hindlimb in mammals, relating the amount of covariation to its role as a constraint on their morphological variation. Similarly, in this paper we identified super-modules as different structures involved in the feeding process and differently constrained by phylogeny and shared ancestry.

METHODS AND MATERIALS

Materials

We took pictures of the skull in the dorsal and lateral views, the mandible in the lateral view, and the upper tooth row in the occlusal view, for all extant rhino species [*Diceros bicornis* (Linnaeus 1758), *Ceratotherium simum* (Burchell 1817), *Dicerorhinus sumatrensis* (Fisher von Waldheim 1814), *Rhinoceros sondaicus* (Desmarest 1822), *Rhinoceros unicornis* (Linnaeus 1758)] plus six extinct species that occur in the Plio-Pleistocene fossil record of Europe [*Stephanorhinus etruscus* (Falconer 1868), *Stephanorhinus jeanvireti* (Guérin 1972), *Stephanorhinus hundsheimensis* (Toula 1902), *Stephanorhinus hemitoechus* (Falconer 1868), *Stephanorhinus kirchbergensis* (Jäger 1839) and *Coelodonta antiquitatis* (Blumenbach 1799)]. Altogether, 179 specimens were analysed. Details about the number of specimens per species and per configuration are provided in Online Appendix I (evolutionary-ecology.com/data/2578Appendix-1.pdf). As for living rhinos, we only included wild specimens, since animals bred in captivity very often show growth abnormalities and bone tissue deformations. We formally eliminated any possible influence of intraspecific allometry (due to sex differences or small age differences) by performing our analyses on shape residuals obtained from species-specific regressions between shape and size.

Geometric morphometrics

Landmarks and semi-landmarks (landmarks only for the upper tooth row; Fig. 1) were digitized on each specimen picture to capture a detailed representation of shape. Type I, II, and III landmarks (Bookstein, 1991) were used. As for the landmarks digitized on the upper tooth row occlusal view, only those points whose homology based on mammalian tooth

structure is recognizable were selected. We followed the recommendations of Marcus *et al.* (2000) and Mullin and Taylor (2002) so as to avoid parallax errors and to maintain uniform measurement error on pictures. Digitization of all images (skulls, mandibles, and upper tooth rows) was carried out with tpsDig2 software (Rohlf, 2005). We used generalized procrustes analysis [GPA (Bookstein, 1991)] to analyse shape. GPA rotates, aligns, and scales landmark configurations to the centroid size [CS = the square root of the sum of squared distances of a set of landmarks from their centroid (Bookstein, 1986)]. Rotation of the scaled and translated landmark sets is achieved by comparison with a reference configuration (the first specimen in the data set was used here). Once the rotation has been completed, a mean shape is calculated and the rotation process repeated using the mean shape as the reference configuration for the sample (including the previous, empirical, reference-specimen configuration). This mean-shape/rotation procedure is iterated to minimize rotation differences between subsequent iterations. Residual differences are to be ascribed to real shape differences plus measurement error. Principal components analysis (PCA) was performed on the shape residuals to identify orthogonal axes of maximal variation. This is the standard procedure in geometric morphometric studies (Adams *et al.*, 2004).

Perez *et al.* (2006) stated that semi-landmarks differ from landmarks because in addition to translating, scaling, and rotating landmarks optimally, the semi-landmark points are slid along the outline curve until they match as well as possible the positions of corresponding points along an outline in a reference configuration (Adams *et al.*, 2004). This is done because the curves or contours should be homologous from subject to subject, whereas their individual points need not be (Bookstein *et al.*, 2002). A separate sliding semi-landmark file was prepared for tpsRelw to distinguish landmarks from semi-landmarks. This way tpsRelw performs the relative warp analysis using sliding-landmark information during computation (see software details at http://life.bio.sunysb.edu/morph/). To check if error in digitization affects the calculation of interspecific shape variance, 10 pictures were randomly selected and re-digitized five times. Then, the difference in morphological disparity (= shape variance) between them was calculated. Finally, 900 bootstrap random sets of the 50 (5×10) pictures were produced and the difference in disparity between replicated sets and random sets compared. If the average distance between the replicated sets is statistically lower than between random sets, we assume error in digitization is not affecting the calculation of interspecific shape variance in our analyses.

Function: hypsodonty index and feeding categories

In ungulates, a hypsodont (= high crowned) molar is considered to be the principal adaptation for feeding on grasses (Feranec, 2007; Janis, 2008), and rhinos are no exception (Mendoza and Palmqvist, 2008). A hypsodonty index (HI) was calculated on upper third molars in both extant and extinct rhinos, by dividing the upper third molar height by width at the tooth base (Guérin, 1980), and by averaging HI values for any species over a number of unworn teeth we measured directly.

Before using HI in all analyses, we verified that it is a good predictor of diet by regressing feeding category (as the dependent variable) against HI (as the independent variable). We used a special class of linear regression, namely ordinal regression (McCullagh, 1980), which takes into account an ordinal dependent variable. The variable diet was coded in ascending order in *grazer*, *mixed feeder*, and *browser* categories, as is usual with ungulates (Fortelius, 1982; Nowak, 1991; Emslie and Brooks, 1999; Mendoza and Palmqvist, 2008). In addition, we performed an ANOVA

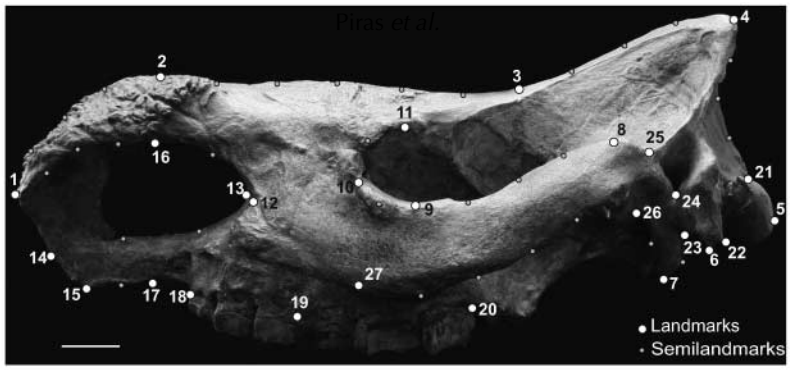
Landmarks
Semilandmarks

(A)

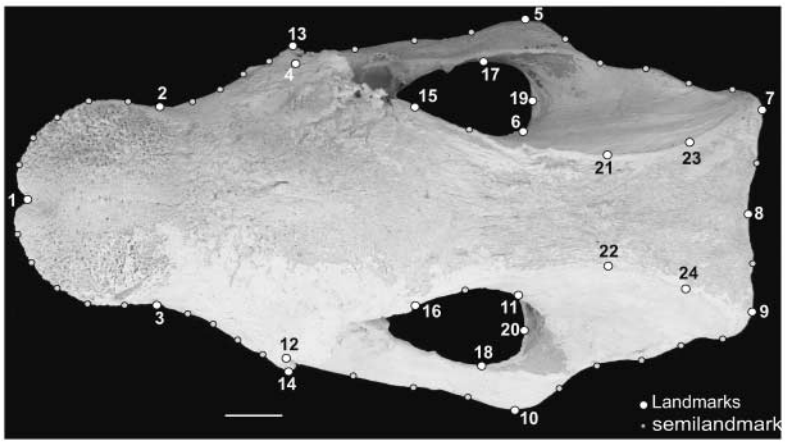
Landmarks
semilandmark

(B)

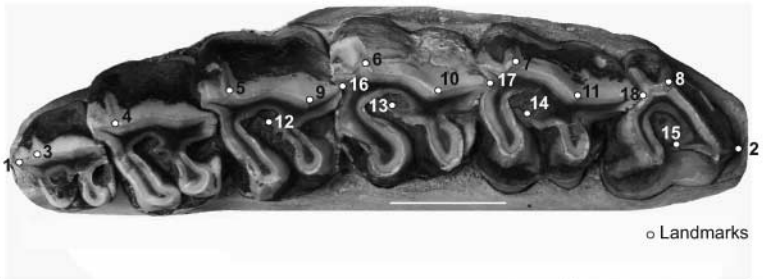
Landmarks

(C)

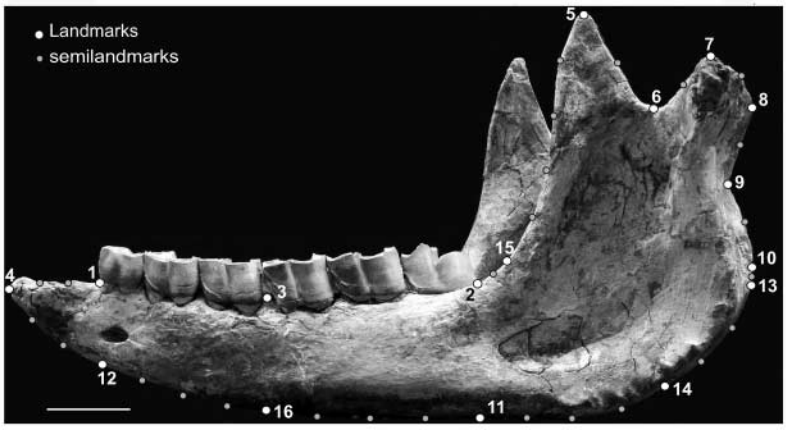
Landmarks
semilandmarks

(D)

using HI as the dependent variable and feeding categories as factor. To take into account phylogeny, we repeated ANOVA with a phylogenetic ANOVA (Garland *et al.*, 1993) implemented in the R-package 'geiger' (Harmon *et al.*, 2009).

For extant species, attribution of feeding category is certain as it is based upon direct observation during feeding (Mendoza and Palmqvist, 2008). For extinct species, feeding category was attributed based on indirect indicators such as cranial morphology, head posture (Loose, 1975; Kahlke and Lacombat, 2008), postcranial features (Fortelius *et al.*, 1993; Lacombat, 2003), and paleoenvironmental data (see Table 1), to avoid the circular argument of inferring diet from HI.

Fig. 1. (A) Landmark configuration of rhino skull in the lateral view (scale bar = 5 cm). 1, Anterior tip of the nasal bones; 2, upper tip of the nasal bones; 3, maximum point of curvature of the frontal-parietal area; 4, maximum point of curvature of the posterior area of the chignon; 5, posterior tip of the occipital condyle; 6, lower tip of the para-occipital apophysis; 7, lower tip of the post-glenoid condyle; 8, upper tip of the zygomatic arch; 9, lower tip of the orbit; 10, anterior tip of the orbit; 11, upper tip of the orbit; 12, infra-orbit foramen; 13, posterior tip of the nasal incision; 14, upper anterior tip of the premaxillary; 15, lower anterior tip of the premaxillary; 16, projection, on the lower side of the nasal, of landmark 2; 17, projection, on the lower side of the premaxillary, of landmark 2; 18, anterior tip of the upper tooth row; 19, posterior tip of the upper premolar row; 20, posterior tip of the upper tooth row; 21, upper tip of the occipital condyle; 22, lower tip of the occipital condyle; 23, anterior tip of the post-tympanic apophysis; 24, lower tip of the acoustic pseudo-meatus; 25, upper concavity of the posterior part of the zygomatic arch; 26, lower concavity of the posterior part of the zygomatic arch; 27, projection, on the lower anterior side of the zygomatic arch, of landmark 10. **(B)** Landmark configuration of rhino skull in the dorsal view (scale bar = 5 cm). 1, Anterior tip of the skull; 2, right concavity of the nasal rugosity; 3, left concavity of the nasal rugosity; 4, anterior tip of the right orbit; 5, right edge tip of the zygomatic arch; 6, maximum right constriction of the parietal; 7, posterior right tip of the occiput; 8, posterior tip of the skull; 9, posterior left tip of the occiput; 10, left edge tip of the zygomatic arch; 11, maximum left constriction of the parietal; 12, anterior tip of the left orbit; 13, lacrimal-caudal right process; 14, lacrimal-caudal left process; 15, right maximum anterior convexity of the medial parietal border of the orbital contour; 16, left maximum anterior convexity of the medial parietal border of the orbital contour; 17, right edge of the orbit contour; 18, left edge of the orbit contour; 19, right posterior tip of the orbit contour; 20, left posterior tip of the orbit contour; 21, maximum right constriction of the parietal crest; 22, maximum left constriction of the parietal crest; 23, right concavity, of the parietal crest, between landmarks 21 and 7; 24, left concavity, of the parietal crest, between landmarks 22 and 9. **(C)** Landmark configuration of rhino upper tooth row (scale bar = 5 cm). 1, Anterior-most tip of the upper tooth row; 2, end of the upper tooth row; 3, apex of paracone fold of P^2; 4, apex of paracone fold of P^3; 5, apex of paracone fold of P^4; 6, apex of paracone fold of M^1; 7, apex of paracone fold of M^2; 8, apex of paracone fold of M^3; 9, mesostylus of P^4; 10, mesostylus of M^1; 11, mesostylus of M^2; 12, crochet of P^4; 13, crochet of M^1; 14, crochet of M^2; 15, crochet of M^3; 16, metastylus of P^4; 17, metastylus of M^1; 18, metastylus of M^2. **(D)** Landmark configuration of rhino mandible (scale bar = 5 cm). 1, Beginning of the lower tooth row; 2, end of the lower tooth row; 3, end of the premolar row (P4) and beginning of the molar row; 4, anterior extremity of the mandible symphysis; 5, upper extremity of the coronoid process; 6, ventral tip of the sigmoid incision; 7, upper extremity of the condyloid process; 8, posterior extremity of the crest of the condyloid process; 9, inflection point of the neck of the condyloid process; 10, posterior extremity of the horizontal branch of the mandible; 11, projection of landmark 2 to the lower edge of the mandible; 12, projection of landmark 1 to the lower edge of the mandible; 13, projection of the line linking landmarks 1–2 to the posterior part of the horizontal branch; 14, vertex of landmarks 11–2–14 of 60°; 15, point of maximum curve of the anterior side of the vertical branch; 16, projection of landmark 3 to the lower edge of the mandible.

Table 1. Assignment of species to feeding categories (the predicted category according to ordinal regression is given in parentheses)

Species	Diet	Inferred from	References
Diceros bicornis	Browser (Browser)	Direct observation	Nowak (1991); Codron *et al.* (2007); Cumming *et al.* (1990); Dierenfeld (1995); www.rhinoresourcecenter.com
Ceratotherium simum	Grazer (Grazer)	Direct observation	Nowak (1991); Codron *et al.* (2007); Cumming *et al.* (1990); Shrader *et al.* (2006); www.rhinoresourcecenter.com
Dicerorhinus sumatrensis	Browser (Browser)	Direct observation	Dierenfeld (1995); www.rhinos-irf.org; www.rhinoresourcecenter.com
Rhinoceros sondaicus	Browser (Browser)	Direct observation	Pratiknyo (1991); www.rhinos-irf.org; www.rhinoresourcecenter.com
Rhinoceros unicornis	Mixed feeder (Browser)	Direct observation	Fortelius (1982); Laurie (1982); Laurie *et al.* (1983); www.rhinoresourcecenter.com
Coelodonta antiquitatis	Grazer (Grazer)	Faunal complex, post-cranial features, paleoenvironment	Fortelius (1982); Lacombat (2003); Kalhke and Lacombat (2008)
Stephanorhinus etruscus	Browser (Browser)	Faunal complex, post-cranial features, paleoenvironment	Fortelius (1982); Fortelius *et al.* (1993); Mazza and Azzaroli (1993); Lacombat (2003)
Stephanorhinus hemitoechus	Mixed feeder (Browser)	Faunal complex, post-cranial features, paleoenvironment	Fortelius *et al.* (1993); Lacombat (2003)
Stephanorhinus hundsheimensis	Browser (Browser)	Faunal complex, post-cranial features, paleoenvironment	Fortelius *et al.* (1993); Mazza and Azzaroli (1993); Lacombat (2003)
Stephanorhinus jeanvireti	Browser (Browser)	Faunal complex, paleoenvironment	Guérin (1980)
Stephanorhinus kirchbergensis	Browser (Browser)	Faunal complex, post-cranial features, paleoenvironment	Fortelius (1982); Loose (1975); Fortelius *et al.* (1993); Lacombat (2003)

Although it might seem odd inferring diet from postcranial material, this procedure reflects known adaptation in the ungulate skeleton to live in different environments exploiting different food items (Owen-Smith, 1988; Spencer, 1995). This is true for rhinos as well (Fortelius *et al.*, 1993; Mazza and Azzaroli, 1993). For instance, head posture, neck length, and the length of the spinal processes of the anterior thoracic vertebrae allow one to differentiate browsing from grazing rhinos. Limb proportions indicate the degree of cursoriality and were used as indicators of feeding behaviour as well, since open habitats are usually covered with grasses (Agusti and Anton, 2002; Lacombat, 2003). Moreover, the fossil associations our rhino species were part of are often indicative of habitat, since many other species were known to be habitat specialists (e.g. woolly rhino often occurs with the woolly mammoth, which was a steppe specialist).

In Table 1 we report attribution of diet category for all of the species analysed here and the references upon which the assignments were made.

Shape–size and shape–hypsodonty index relationships

For each landmark configuration (skull in dorsal and lateral views, mandible in lateral view, and upper tooth row in the occlusal view), separate multivariate regressions between Procrustes shape coordinates (dependent variables) and HI (independent variable) were performed, to assess global morphological changes associated with HI. The same procedure was performed using size (logCS) as an independent variable to explore morphological variation associated with *interspecific* size differences (intraspecific differences were formally removed by using residuals of per-species regressions between shape and size). MorphoJ (Klingenberg, 2011) was used to perform multivariate regressions. Its algorithm returns a vector of regression scores for shape that represents the shape correlated the most with the independent variable (HI or size).

Phylogeny

A phylogenetic tree including all species studied here (Fig. 2) was built in Mesquite 2.5 (Maddison and Maddison, 2007). For the extant rhinoceroses, recent papers based on genetic distances (Tougard *et al.*, 2001; Orlando *et al.*, 2003; Prithiviraj *et al.*, 2006), from which we retain the tree topology, were used. Branch lengths were calibrated in millions of years (Ma) based on the fossil record. For topological, geographical, and biochronological information concerning the extinct rhinoceroses of the genus *Stephanorhinus*, we used the tree topology proposed by Lacombat (2003); for the genus *Dihoplus*, we followed Heissig (1989) and Giaourtsakis *et al.* (2006); for *Coelodonta*, we followed Kahlke and Lacombat (2008); and for the tribe Elasmotheriina, we followed Antoine (2002). For the African genera *Ceratotherium* and *Diceros*, we followed Cerdeño (1998) and Geraads (2005). For the Asiatic genera *Dicerorhinus* and *Rhinoceros*, we followed Groves and Kurt (1972), Tong (2001), Nanda (2002), and Louys *et al.* (2007).

Phylogenetic comparative methods

In comparative studies of organisms' traits, the observations are rarely independent of each other because of phylogenetic relationships (Felsenstein, 1985; Harvey and Pagel, 1991; Garland *et al.*, 1992). To take into account the non-independence of data points due to phylogeny, a number of comparative methods have been proposed in the literature. Most of these have their

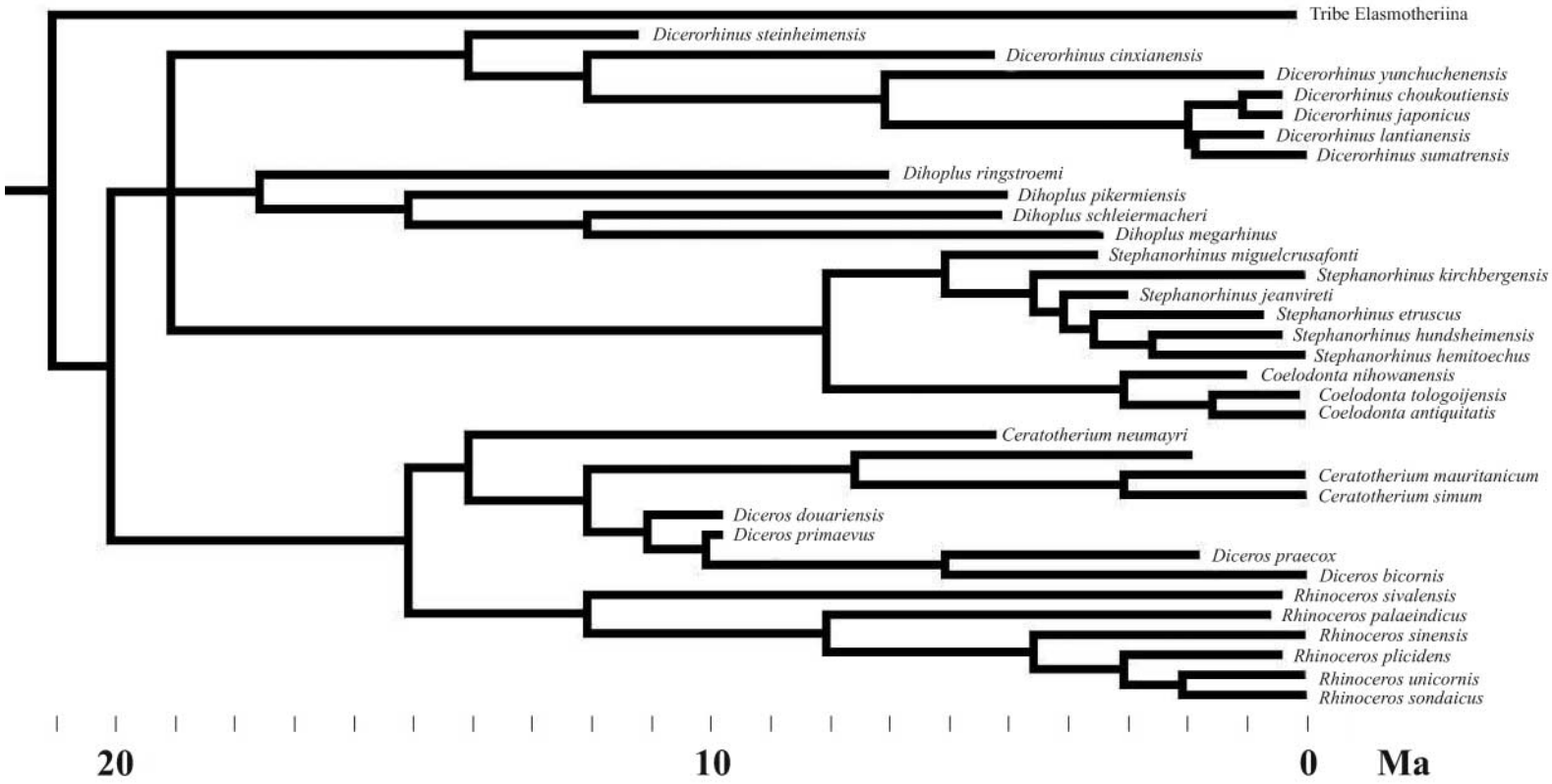

Fig. 2. Phylogenetic tree used for this study. Scale is in millions of years (Ma).

pros and cons (Martins *et al.*, 2002; Garland *et al.*, 2005; Lavin *et al.*, 2008), consequently it is advisable to adopt more than one method at any time (Garland *et al.*, 2005). We followed this recommendation and applied both phylogenetically independent contrasts (PICs) and variation partitioning (VARPART).

Since Felsenstein's (1985) seminal paper, PICs represent the main comparative method (Garland, 1992). Rohlf (2001, 2006) demonstrated that PICs are a special case of phylogenetic generalized least squares (PGLS) regression. In generalized least squares (GLS) regression, a known (or hypothesized) covariance matrix of the residuals on the dependent variable Y is used to back-transform the regression variables and estimate regression coefficients anew. In comparative studies, the structure of residuals is the tree-based phylogenetic variance–covariance matrix, and GLS is explicitly defined as 'phylogenetic' (hence PGLS). Thus, PGLS draws from the tree topology and branch lengths the variance–covariance matrix of the error term ε in the regression equation $Y = \beta X + \varepsilon$, assuming evolution proceeds based on a Brownian motion model. Brownian motion represents fluctuating selection with constant trait variance (Rohlf, 2001, 2006; Blomberg *et al.*, 2003; Adams, 2008; Lavin *et al.*, 2008). The initial regression equation is then transformed via the GLS procedure as $Y' = \beta X' + \varepsilon'$, which has uncorrelated errors with equal variance (Rohlf, 2001, 2006). PICs, computed in MorphoJ 1.01b (Klingenberg, 2011) for shape (Procrustes coordinates previously aligned using semi-landmarks), HI, and logCS, were averaged by species and compared with ordinary least squares regression models (OLS).

Variation partitioning [VARPART (Desdevises *et al.*, 2003)] is a development of phylogenetic eigenvector analysis [PVR (Diniz-Filho *et al.*, 1998)] based on partial regressions. The rationale underlying VARPART is to extract a set of continuous variables from a given phylogeny to be used in standard regression analyses so as to assess the dependent variable's variance due to phylogeny as in common multiple regression. This is done by first computing the distance matrix between taxa based on branch lengths and then by performing a principal coordinates analysis on this matrix to extract a set of orthogonal continuous variables (PCoords). Rohlf (2001) criticized matrices based on path length distances of the type used here, stating that they do not represent the expected amount of independent evolution since divergence from a common ancestor, although ultrametric and path length distances are usually *highly correlated* (Rohlf's words in italics). We do not believe that the height above the tree root of the common ancestor is the most appropriate metric when the phylogenetic tree is not ultrametric because species in a pair may have very unequal duration (for example, in our case, by more than 4 Ma). Thus, by using covariance between species pairs, we can ignore that these two species could have had very different periods of time to evolve their shapes.

Diniz-Filho *et al.* (1998) proposed using the broken-stick model (Frontier, 1976) to select PCoords. Rohlf (2001) and Martins *et al.* (2002) noted that this approach does not allow one to take the entire phylogeny into account. Desdevises *et al.* (2003) similarly criticized the broken-stick criterion and alternatively proposed testing principal coordinates individually to determine their influence on the dependent variables. In keeping with this criticism, we retained here all the PCoords that explained at least 95% of the cumulative variance. We emphasize, however, that using PCoords that explained up to 99.9% of variance returned identical results.

Borcard *et al.* (1992) and Desdevises *et al.* (2003) proposed a method to partial out the interactions between different sets of variables during a multiple multivariate regression that can be summarized as follows: Y is the dependent variable, here represented by shape

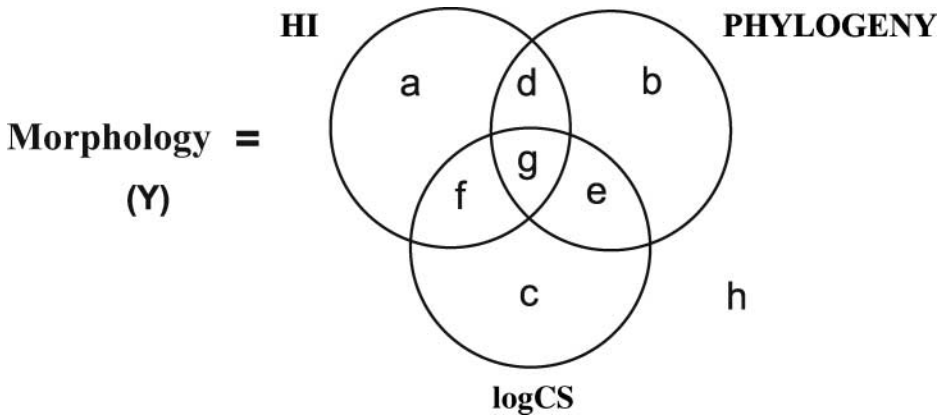

Fig. 3. Decomposition scheme for the variation partition analysis explained in the text.

(i.e. all non-zero PCs), X_1 represents an independent variable (here HI), X_2 stands for the PCoords explaining at least 95% of total variance, and X_3 represents $\log_{10}$ centroid size (logCS). First, a regression of Y on X_1 is computed. The coefficient of (multiple) determination of the regression, R^2, is equal to the fraction $a+d+f+g$ in the decomposition scheme in Fig. 3. Second, Y is similarly regressed on X_2 and X_3. Here R^2 is equal to fractions $b+d+e+g$ and $c+e+f+g$ of the decomposition scheme in Fig. 3. Then, Y is regressed on all independent variables; the resulting R^2 is equal to the fit of the entire model. The individual values of fractions a, b, and c can be obtained by subtraction from the previous results. The 'overlap' fraction $f+g$ is the phylogenetically structured functional variation (Cubo *et al.*, 2005). After obtaining these individual fractions, the residual variation can be estimated by $d=1-(a+b+c+d+e+f+g)$. It is then possible to obtain the fitted values corresponding to fractions a, b, and c. For example, for a it is necessary to compute a partial regression of Y on X_1, using X_2 and X_3 as covariates. The R^2 computed this way corresponds to fraction a, and can be tested for significance. Fraction c is similarly obtained by partial regression of Y on X_3, using X_1 and X_2 as covariates. The overlap fractions (including the phylogenetically structured functional variation, $d+e+f+g$) can only be obtained by subtraction. Hence, it is not possible to test them for significance (Borcard *et al.*, 1992). Further details about the individual steps of the variation partitioning method can be found in Desdevises *et al.* (2003) and Cubo *et al.* (2008). In multiple multivariate regressions, the R^2 is flawed due to the unequal number of variables per explanatory factor. Factors including more variables will have higher R^2 (Ohtani, 2000). In the present study, because phylogeny as a factor includes more variables than HI or logCS, we would overestimate the importance of phylogeny in regressions against shape. Consequently, we used adjusted R^2 coefficients, which account for overfitting and produce unbiased estimates of the fractions of variation of the response variable explained by each factor (Peres-Neto *et al.*, 2006; Ramette and Tiedje, 2007).

Variation partitioning was computed by using the library 'vegan' (Oksanen *et al.*, 2008) for R (R Development Core Team, 2010). The Stratigraphic tool module (Josse *et al.*, 2006) was used to produce the phylogenetic distance matrix (D) to be exported and successively analysed with PCO3 software (Anderson, 2003).

Morphological integration

We tested that the shape configuration (module) most influenced by pure HI (and the least by pure phylogeny; see below) was less integrated with the others. Integration and modularity are studied by analysing the covariation among modules. Here we used a metric of covariation between the various sets of variables: the *RV* coefficient (Escoufier, 1973). This coefficient was originally proposed by Escoufier (1973) as a measure of the association between two sets of variables (e.g. X and Y): $RV = \mathrm{tr}(Y'XX'Y)/\{\mathrm{tr}[(X'X)2]\,\mathrm{tr}[(Y'Y)2]\}1/2$ (where X and Y are the Procrustes coordinates matrices of the different modules, and tr indicates the trace of a matrix). The *RV* coefficient is analogous to the *R*-square in the univariate case (Claude, 2008). The equation for calculating *RV* therefore represents the amount of covariation scaled by the amount of variation within the two sets of variables, which is analogous to the calculation of the correlation coefficient between two variables (Klingenberg, 2009). *RV* may take any value from 0 to 1.

RESULTS

Geometric morphometrics

The difference in disparity between replicated sets is statistically lower than between random sets (mandibles, simulated $P = 0.045$; skulls, simulated $P = 0.025$; teeth, simulated $P = 0.030$). This means that error in digitization does not have a significant effect on shape analysis.

In the four configurations, the first 15 principal components explain collectively some 95% of total shape variance. Figure 4 shows the relationships between PC1 and PC2 for each of the four configurations. In the lateral skull view, a strongly concave and dolicocephalic skull with a shallow nasal incision corresponds to low PC1 values, whereas at high values the skull is less concave, with a backward shifted occiput and deep nasal incision. At positive PC2 values, the nasal bone becomes more and more bulky as the nasal incision is less pronounced. At the same values, the premaxilla is short and the orbit low. In the dorsal skull view, along PC1 the skull occiput becomes more and more massive, as do the nasal and parietal bones. High values in PC2 are associated with long and slender nasal bones and a short occiput. Regarding morphology of the mandible, along PC1 the horizontal ramus becomes slender as the ascending ramus shortens. On PC2 the horizontal ramus assumes a convex profile and the ascending ramus inclines posteriorly as one moves from low to high scores. Finally, the upper tooth row becomes slender, shows more developed crests on the buccal side, and proportionally smaller M^3 as one moves towards positive scores along PC1. Along PC2, the tooth row shows labially shifted crochets and appears more curved.

Relationship between hypsodonty index and feeding categories

Ordinal regression between HI and feeding categories is significant ($P \ll 0.001$; Cox and Snell pseudo $R^2 = 0.36$). Predicted diet categories are show in Table 1. While grazers and browsers are correctly classified, the mixed feeders are classified as browsers. The ANOVA is significant ($P = 0.022$) as well as the phylogenetic ANOVA ($P = 0.009$). Thus, we can assume that HI is a good predictor of feeding habits for extant and extinct rhinos and can be used in the following statistical analyses.

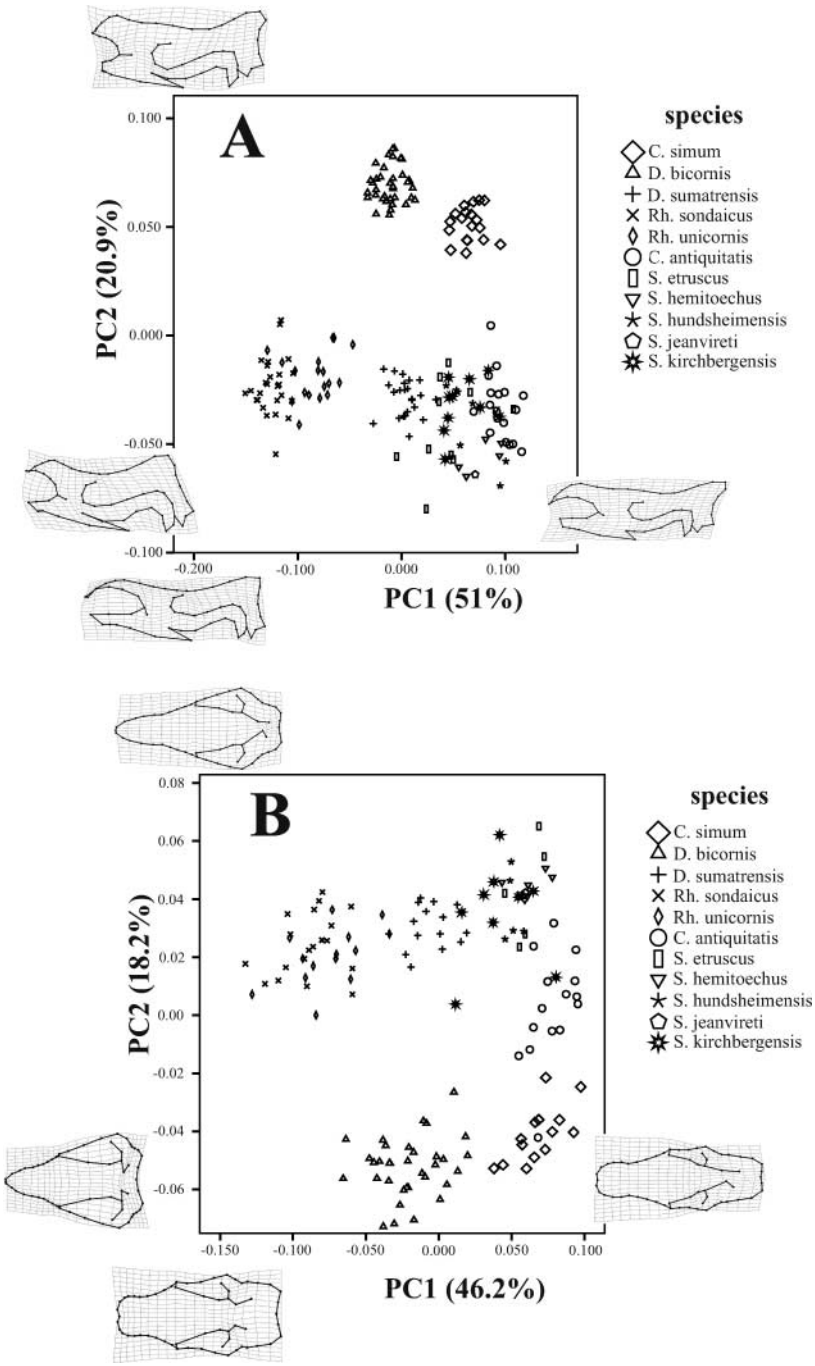

Fig. 4. Scatterplots between PC1 and PC2 for the four configurations: (A) skull in lateral view, (B) skull in dorsal view, (C) mandible, (D) upper tooth row. Deformation grids refer to PC axis extremes (positive and negative). The percentages of total variance explained are given in parentheses.

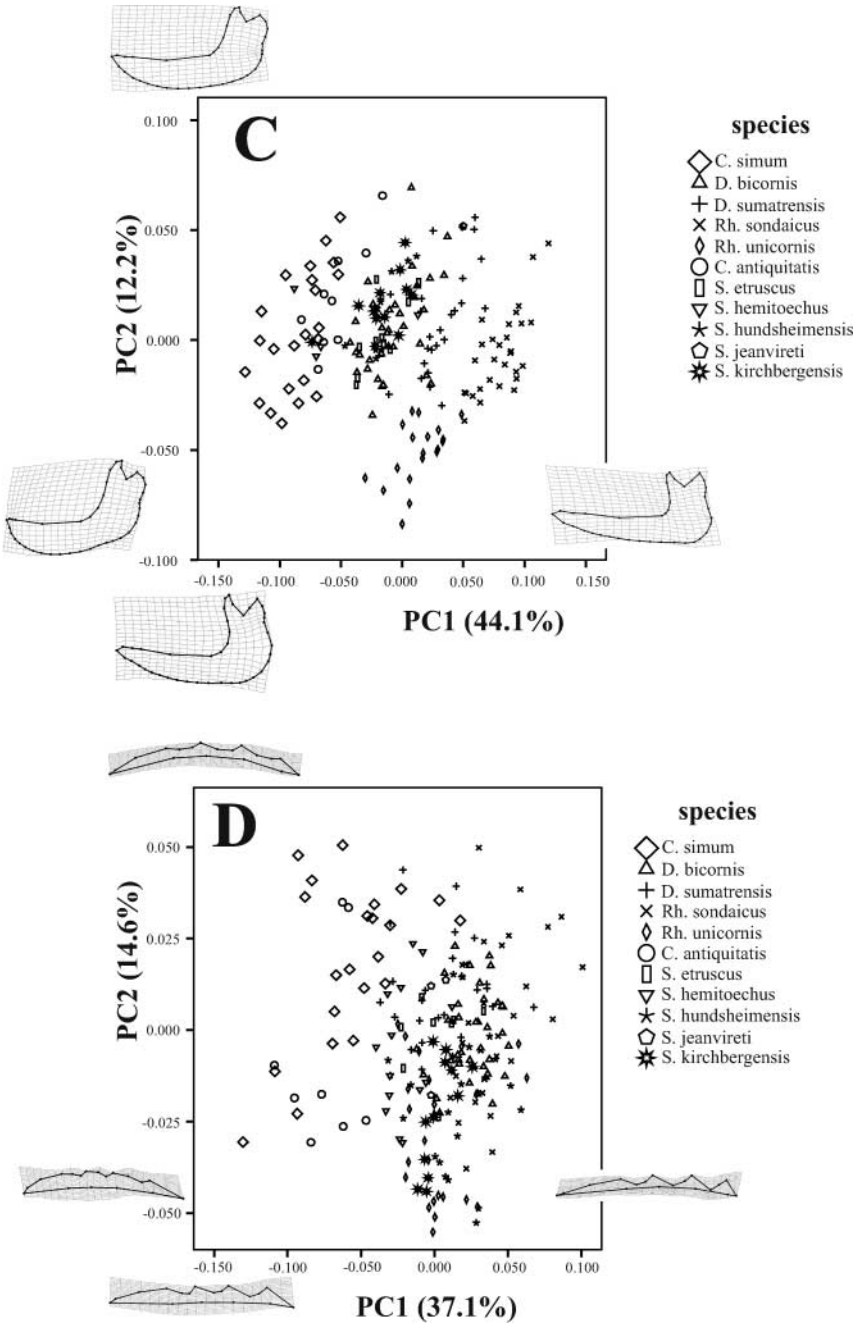

Fig. 4. *Continued.*

Shape–size and shape–hypsodonty index relationships

For the dorsal skull view, multivariate regression between shape variables and logCS is significant (Wilks' lambda = 0.36; $P = 0.003$). Goodall's *F*-test revealed that size explains 12.95% of shape variance. Figure 5A shows morphological changes in skull dorsal view that are associated with HI. Larger size implies a massive skull with a well-developed occiput, strongly developed nasal-parietal bones, and proportionally smaller orbits. Multivariate regression between shape variables and HI is significant (Wilks' lambda = 0.0014; $P \ll 0.001$). Goodall's *F*-test indicates that HI explains 20.78% of shape. Major changes associated with high HI values are a strongly developed occiput and a short and large nasal-parietal portion of the skull.

For the lateral skull view, multivariate regression between shape variables and logCS is significant (Wilks' lambda = 0.24; $P = 0.009$). Goodall's *F*-test indicates that size explains 12.73% of shape variance. Major changes associated with larger size are the occiput well developed posteriorly, massive nasal bones, a deep nasal incision, and a proportionally shorter tooth row. Figure 5B shows morphological changes in skull lateral view that are associated with HI. Multivariate regression between shape variables and HI is significant (Wilks' lambda = 0.014; $P \ll 0.001$). Goodall's *F*-test indicates that HI explains 22.65% of shape variance. Major changes associated with high HI values are the occiput well developed posteriorly, massive and short nasal bones, a shallow nasal incision, and a low placement of the orbit in the skull.

For the mandible (Fig. 6A), multivariate regression between shape variables and logCS is significant (Wilks' lambda = 0.30; $P \ll 0.001$). Goodall's *F*-test indicates that size explains 15.55% of shape variance. Major changes associated with small size imply a relatively longer tooth row, and a long and slender horizontal ramus. Multivariate regression between shape variables and HI is significant (Wilks' lambda = 0.062; $P \ll 0.001$). Goodall's *F*-test indicates that HI explains 25.52% of shape variance. Figure 6A shows morphological changes in mandible morphology associated with HI. Major changes associated with high HI values are a large mandible showing a well-developed concave profile along the ventral edge of the horizontal ramus and posterior to the ascending ramus.

For the upper tooth row occlusal view (Fig. 6B), multivariate regression between shape variables and logCS is significant (Wilks' lambda = 0.46; $P = 0.0001$). Goodall's *F*-test test reveales that size explains 3.69% of shape. Major changes associated with large size are represented by the loss of saw-like morphology of the tooth row with the labial edges of P^4, M^1, and M^2 being slightly flattened (Fortelius, 1981, 1982). Multivariate regression between shape variables and HI is significant (Wilks' lambda = 0.1117; $P \ll 0.001$). Goodall's *F*-test revealed that HI explains 15.92% of shape. Figure 6B shows morphological changes in the upper tooth row associated with HI. Major changes associated with high HI values include a slightly squared profile with the labial edge of P^4, M^1, M^2, and M^3 slightly flattened labially.

Comparative methods

Table 2 shows results of OLS and PICs regressions performed on shape–HI and shape–logCS relationships for the four configurations. All relationships are significant in the PICs regressions except for the shape–HI relationship in the skull dorsal view and the shape–size relationship in the upper tooth row. Starting from this, to explore the differential contribution of HI and phylogeny we applied VARPART to separate pure from entire

fractions of HI, phylogeny, and size simultaneously. Figure 7 shows the results of the VARPART analyses for the four configurations. Details of all fractions are given in Online Appendix 2 (evolutionary-ecology.com/data/2578Appendix-2.pdf).

The two methods returned consistent results, indicating a strong influence of phylogeny and a weaker influence of pure HI on skull morphology; and a strong influence of pure HI on the mandible and on the upper tooth row. In particular, pure HI is higher for the mandible and slightly smaller for the upper tooth row, while pure phylogeny presents a decreasing gradient from skull to mandible to upper tooth row.

Morphological integration

As anticipated, the configuration (module) showing the strongest influence of pure HI is least integrated with the other configurations (Table 3). Thus, the upper tooth row configuration shows the smallest *RV* coefficients on average. Covariation of the tooth row with the mandible is higher than with the skull. All the configurations covary significantly, however, indicating some degree of integration within these parts, despite the different effects that HI and phylogeny have on them.

Table 2. OLS and PICs analyses for shape–HI and shape–size relationships

	OLS % predicted (*P*-value)	PICs % predicted (*P*-value)
Shape–HI relationship		
Skull, dorsal view	17.5 (0.12)	18.4 (0.053)
Skull, lateral view	17.5 (0.13)	28.2 (0.006)
Mandible	26.6 (0.03)	43.5 (0.001)
Upper tooth row	29.4 (0.038)	29.9 (0.01)
Shape–size relationship		
Skull, dorsal view	18.1 (0.12)	21.6 (0.039)
Skull, lateral view	18.47 (0.11)	30.5 (0.027)
Mandible	31.9 (0.007)	64.4 (0.0001)
Upper tooth row	5.26 (0.7)	13.6 (0.35)

Table 3. *RV* coefficients (below the diagonal) and the associated simulated *P*-values after 10,000 permutations (above the diagonal) for testing covariation between module shapes

	dv	lv	mand	ut
dv	1	<0.001	<0.001	<0.001
lv	0.868	1	<0.001	<0.001
mand	0.677	0.694	1	<0.001
ut	0.505	0.441	0.519	1

Note: dv = skull, dorsal view; lv = skull, lateral view; mand = mandible, lateral view; ut = upper tooth row, occlusal view.

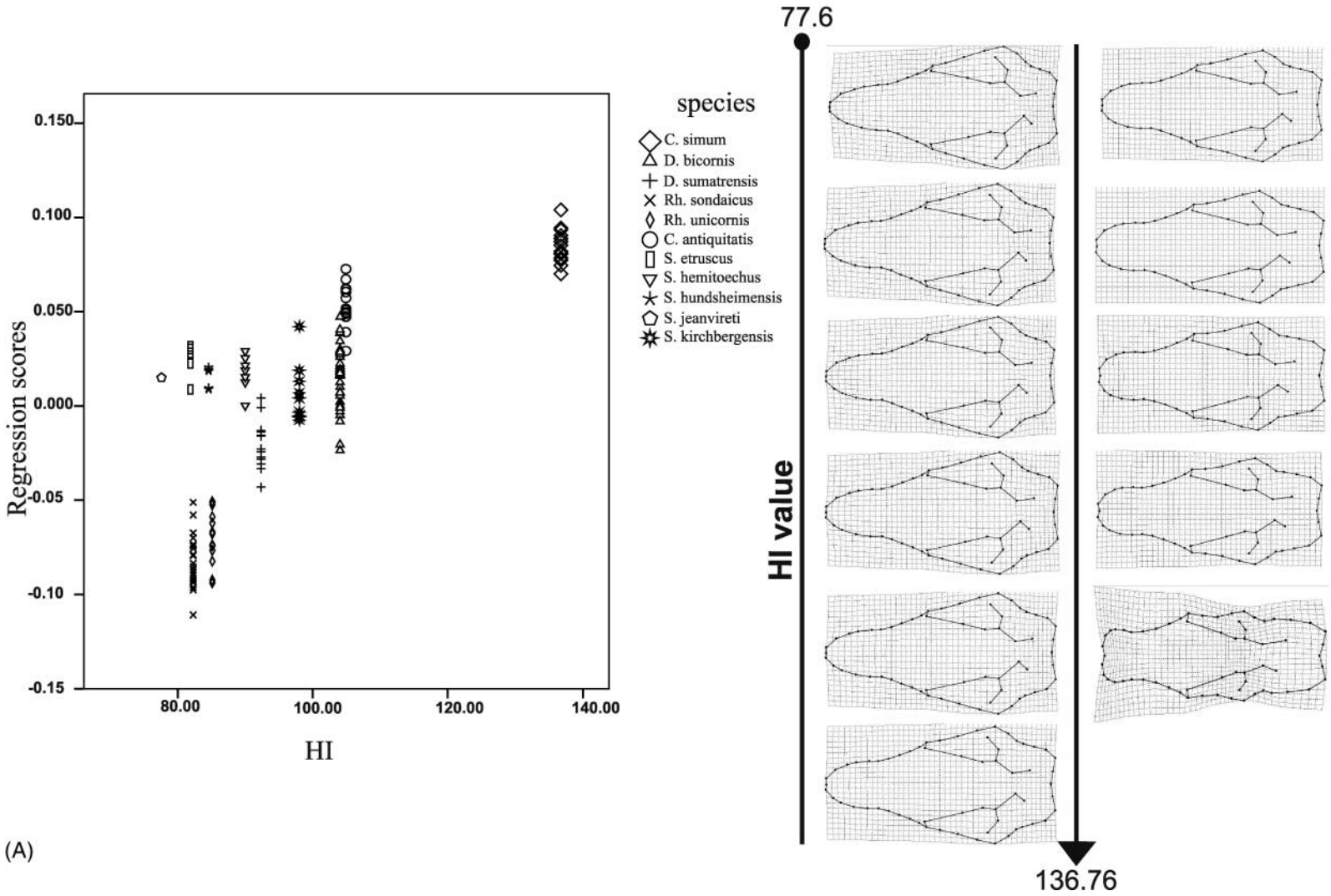
Regression scores
0.150
0.100
0.050
0.000
-0.05
-0.10
-0.15
80.00
100.00
120.00
140.00
HI
species
C. simum
D. bicornis
D. sumatrensis
Rh. sondaicus
Rh. unicornis
C. antiquitatis
S. etruscus
S. hemitoechus
S. hundsheimensis
S. jeanvireti
S. kirchbergensis
77.6
HI value
136.76

(A)

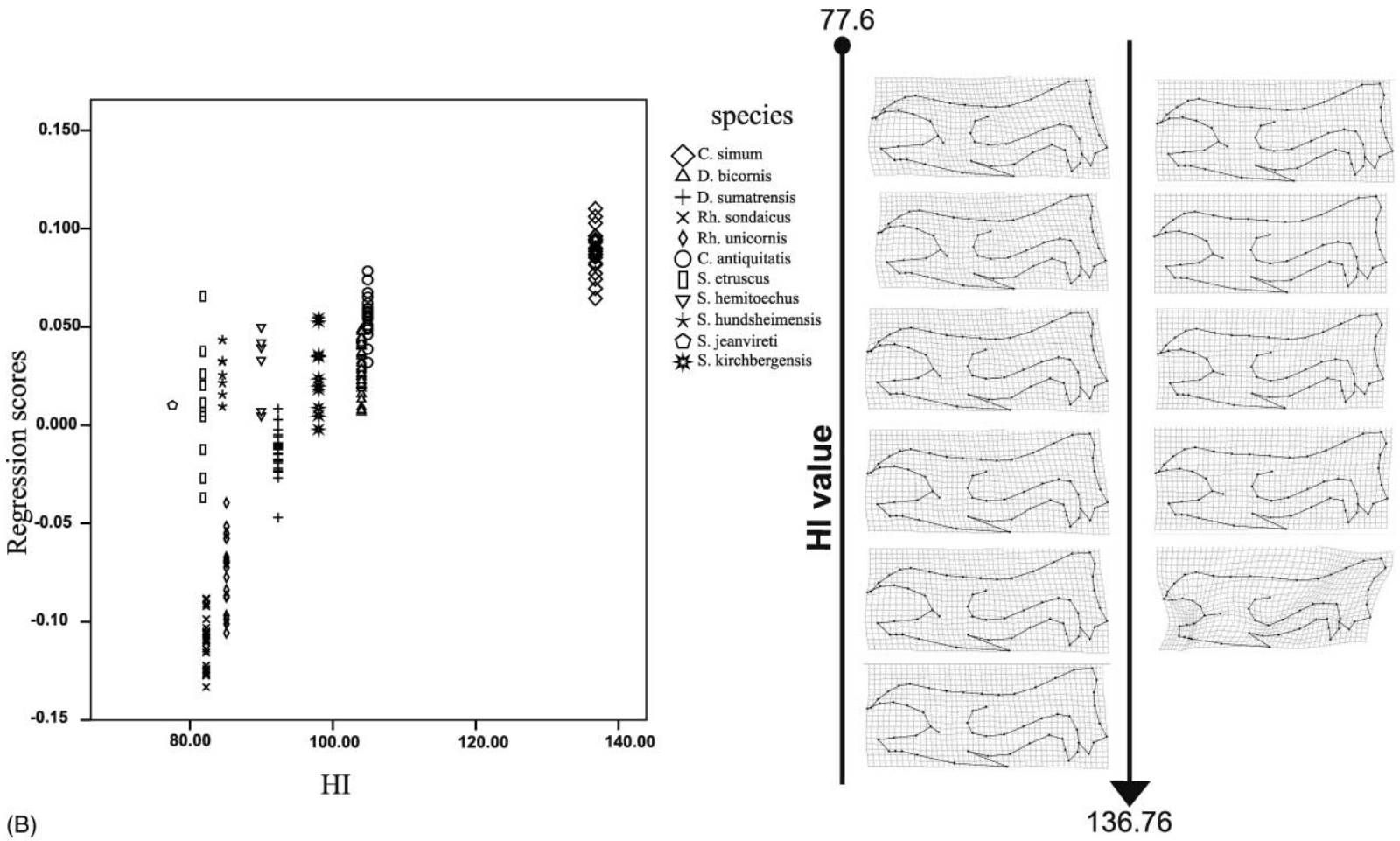

Fig. 5. Scatterplot between regression scores of shape and HI and associated shape changes. (A) Skull in dorsal view, (B) skull in lateral view.

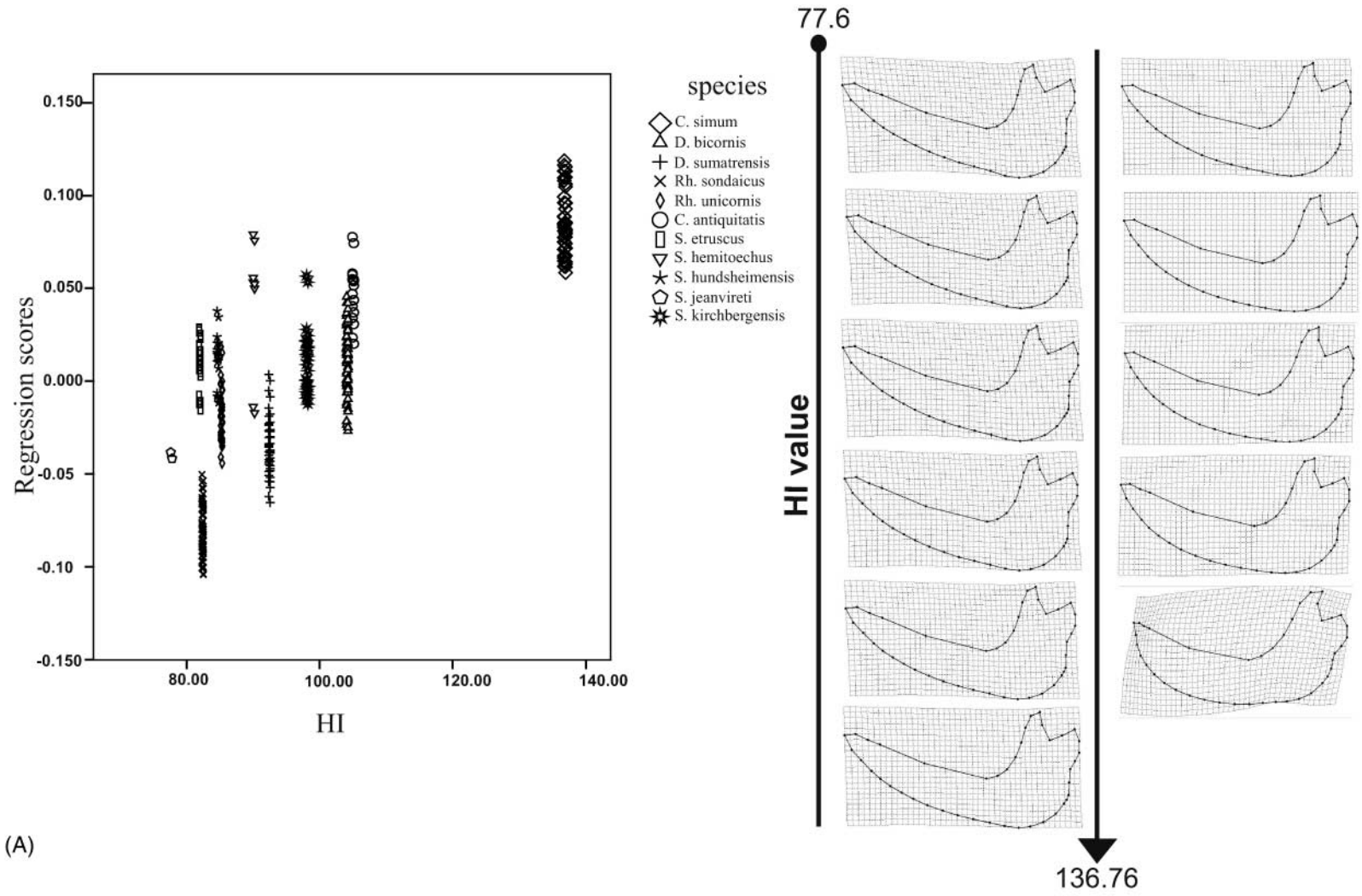
0.150
0.100
0.050
0.000
-0.05
-0.10
-0.150
Regression scores
80.00
100.00
120.00
140.00
HI
species
C. simum
D. bicornis
D. sumatrensis
Rh. sondaicus
Rh. unicornis
C. antiquitatis
S. etruscus
S. hemitoechus
S. hundsheimensis
S. jeanvireti
S. kirchbergensis
77.6
HI value
136.76

(A)

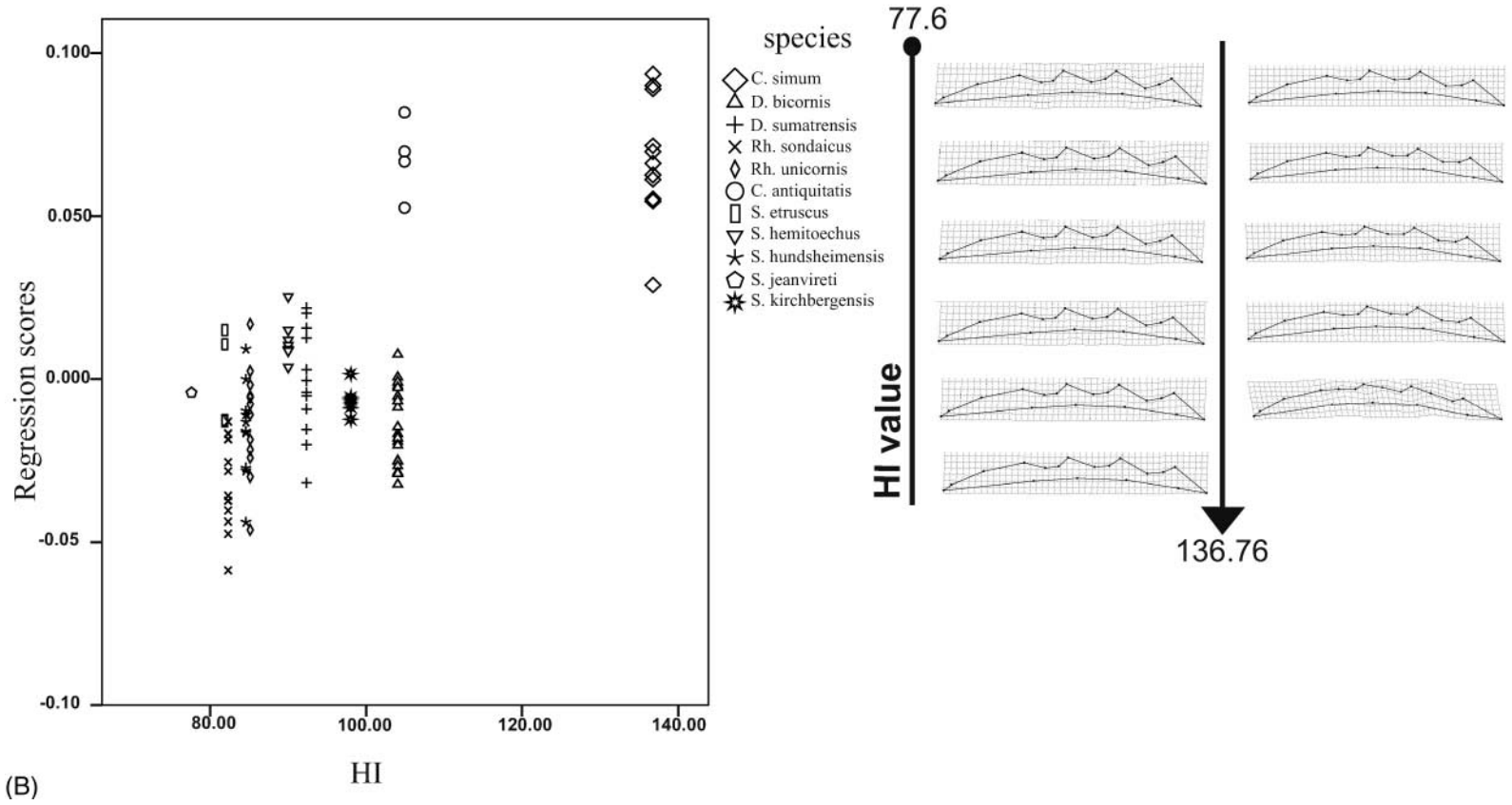

Fig. 6. Scatterplot between regression scores of shape and HI and associated shape changes. (A) Mandible, (B) upper tooth row.

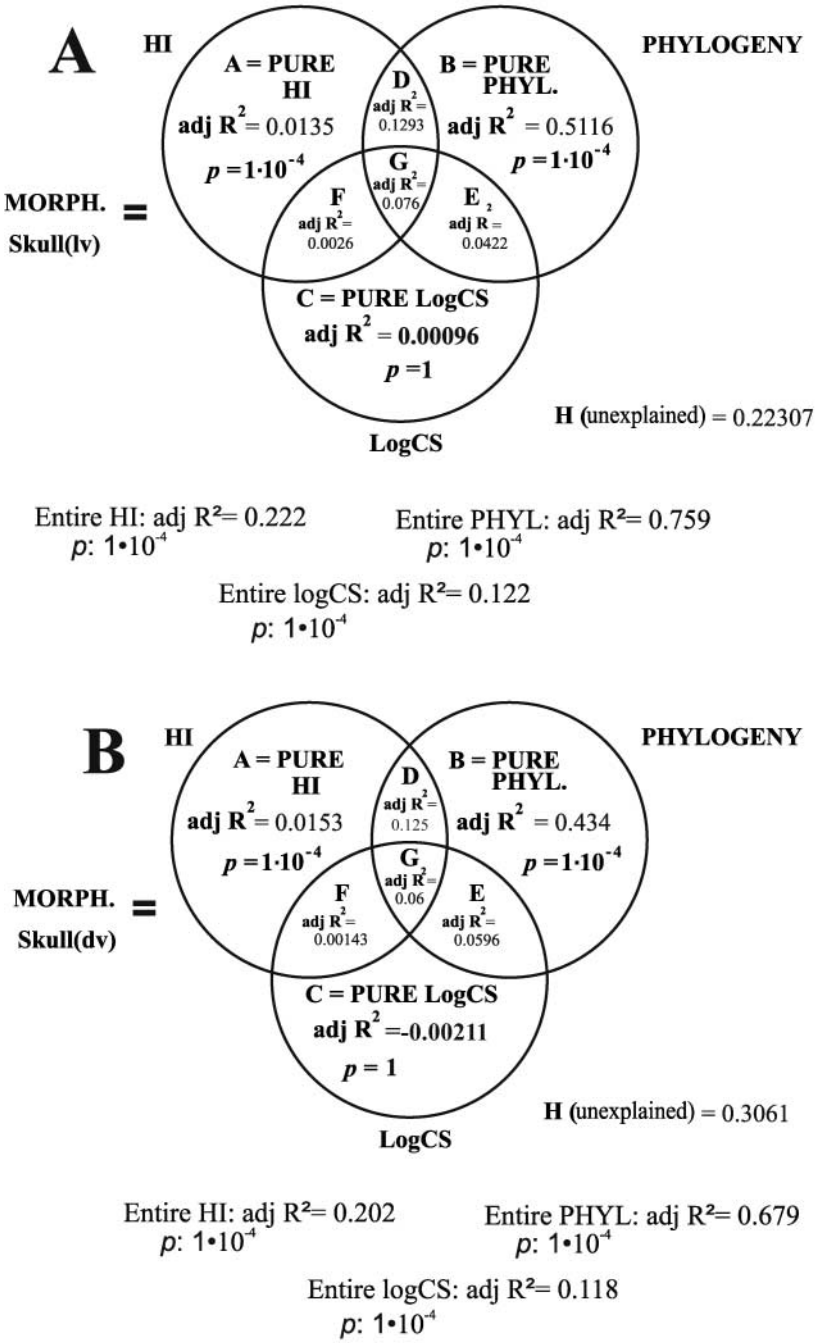

Fig. 7. VARPART results for the four configurations.

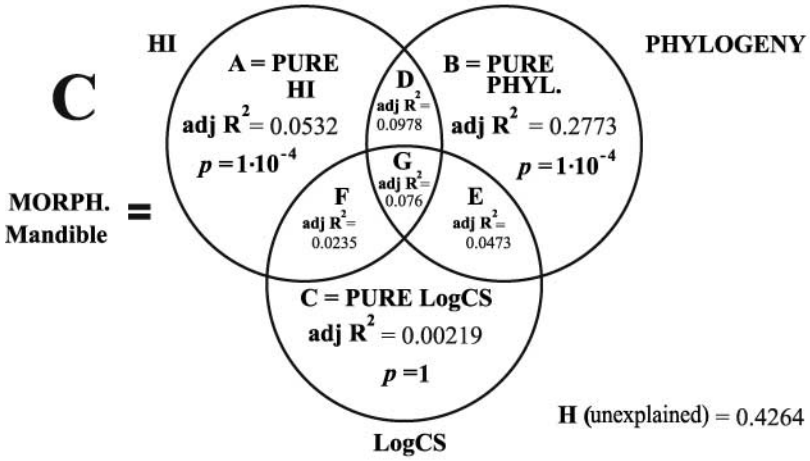

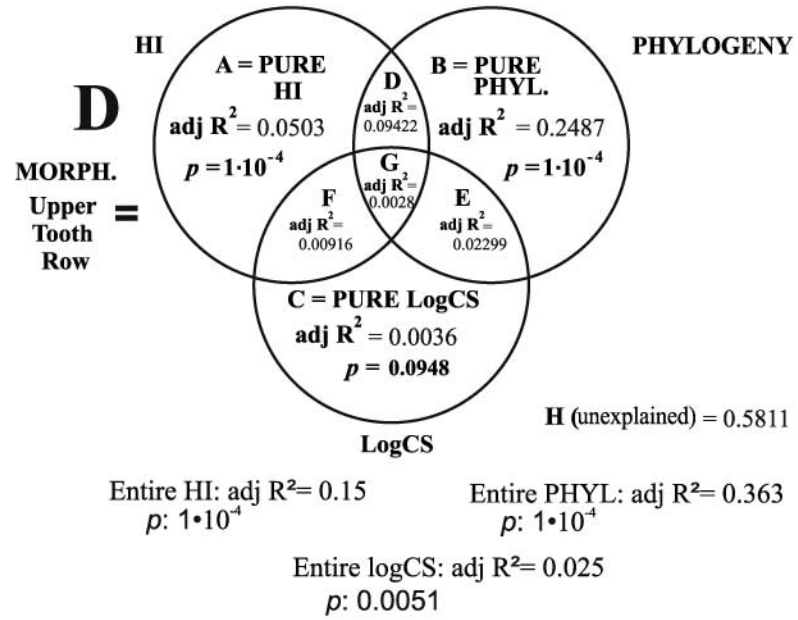

Fig. 7. *Continued.*

DISCUSSION

Once the phylogenetic covariation between operative taxonomic units (i.e. species in our case) is accounted for, the shape–HI relationship is significant for all configurations except for the skull dorsal view. Biologically, this suggests that an association exists between cranial shape and relative crown height.

By applying VARPART, we may further explore this relationship by testing phylogeny and HI in isolation as explanatory factors of shape variance. Phylogeny has the largest influence on shape variance in all configurations. However, a progressive decrease of the variance explained by the *pure* phylogenetic fraction, and a progressive increase from the skull to the upper tooth row and the mandible in the variance explained by the *pure* HI fraction is apparent. These results suggest that feeding adaptation has a greater influence on those structures directly involved in food processing (i.e. the mandible and the tooth row) once the effect of phylogeny is partialled out.

An opposite pattern emerges when looking at the pure phylogeny fraction. This is largest in the dorsal and lateral skull views. This suggests that the upper tooth row and the mandible were less constrained by shared ancestry. VARPART results show, however, that the 'entire' HI fraction (of shape variance explained) is largest with the mandible and then the skull compared with the upper tooth row. On the other hand, skull shape changes are strongly phylogenetically structured. Moreover, it should be noted that given the difficulties in identifying homologies in grazers' and browsers' upper tooth rows, we choose their landmark configuration with 'parsimony' and it is probable that our results underestimate the relationship between upper tooth row shape and HI. In fact, when looking at the upper tooth rows of grazers and browsers, dramatic differences are evident. If the two morphotypes need to be contrasted in a common morphospace, only a conservative configuration can be digitized for both morphotypes. Taking this into account, we suggest that pure HI should covary with upper tooth row morphology even more than observed here.

The overlapping fractions of VARPART between phylogeny and HI deserve particular attention. This fraction is the phylogenetically structured functional variation (PSFV) (Westoby *et al.*, 1995; Desdevises *et al.*, 2003; Cubo *et al.,* 2005). In Fig. 7, PSFV is represented by the fraction $d + g$ in all four configurations. It relates to conserved synapomorphies with functional implications, in contrast to labile, convergent traits that have functional significance only. From our results it is evident that craniofacial morphology and muscle orientation are tightly linked to feeding adaptation. But adaptation (as reflected in HI) and phylogeny are strongly related in the skull (about 19–20% of shape variance explained by PSFV; see Figs. 7A and B). For the mandible, this interaction is slightly weaker (some 17% of variance explained; Fig. 7C). Upper tooth row is the configuration with the smallest PSFV value (~7%) compared with the other anatomical areas. These results suggest that HI is highly phylogenetically structured in the skull (and slightly less so in the mandible), reflecting shared synapomorphies (Raia *et al.*, 2010). Tooth row, in contrast, appears to be the least influenced structure by the phylogenetic structured functional variation.

Morphology of the upper tooth row profile becomes saw-like shaped in browsers due to the rostrocaudal alignment of the paracone, mesostylus, and metastylus, while in grazers it is more rounded. We argue that the upper tooth row morphology lost the saw-like profile in grazers because of the abrasive grasses they feed on [as suggested by Fortelius (1982), among others]. This feature profoundly modified the grazing rhino dentition, whose rate of consumption during feeding is much higher than that of browsers (Fig. 6B).

Bales (1996) suggested that adaptation to either grazing or browsing significantly affects skull anatomy in rhinos because of the different functional demands the skull muscles exert on the mandible and on the occipital portion of the skull. Grazers and browsers have different head postures (Owen-Smith, 1988), with the head being lowered in grazers (Figure 9 in Bales, 1996). The occiput is shifted backward and the occipital plate is oriented differently in grazers (Fortelius *et al.*, 1993; Bales, 1996; Lacombat, 2003). This implies a larger suspensory role for the posterior temporalis that is counteracted by the orientation of the masseter muscle. In grazers, the latter has a small vertical component, since the mandible does not need to be suspended against gravity due to its lowered position (i.e. the momentum of the mandible lever arm is smaller in grazers). In terms of mandible morphology, the outcome of this muscular geometry produces proportionally longer horizontal rami in browsers (see Fig. 6A). As stated earlier, a raised head position implies a forward inclined occipital profile (which occurs in browsers). From a biomechanical point of view, this morphology allows a better lever for neck muscles.

The prediction that the module that is *simultaneously* correlated the most with (pure) HI and the least with (pure) phylogeny should be less integrated with the other modules was confirmed by our results. The *RV* coefficients indicate that the upper tooth row is less integrated with the skull and mandible than the latter are to each other. This suggests that the upper tooth row shape has been driven more by adaptation to current conditions (not phylogenetically structured) than by shared ancestry due to phylogenetic relationships, compared with any other structure shape considered here. Morphological integration predicts that strongly covarying modules will co-evolve because of their coordinated response to selection. Functional integration is expected to occur when the modules share a common function (Cheverud, 1996). This integration can be thought of as a relative constraint, since tightly integrated parts are less able to respond to independent selective pressures (i.e. they possess less evolvability). This reduction in evolvability is not irreversible, since a reduction in functional and hence developmental interactions among modules may occur under selection for functional specialization (Hallgrímsson *et al.*, 2002). In the history of ungulates, a major change in selection regime for feeding occurred with the spread of grasslands in the Miocene (Janis, 2008). Browsing, and the possession of low-crowned molars, is the plesiomorphic condition for the clade, and for rhinos as well. The acquisition of hypsodont molars served as the primary adaptation to exploitation of grass. Here we dissected the nature of the phenotypic response to grazing in rhinos, and found that the (upper) tooth row is the most evolvable structure in the cranium, with a cascade of phenotypic effects descending in intensity from the teeth to the mandible [whose phenotypic response is architecturally mediated by the requirement to house longer teeth roots (Raia *et al.*, 2010)] to the skull. This suggests that teeth are the most evolvable structure in rhino crania, as previously found in carnivores (Dayan *et al.*, 2002).

CONCLUSIONS

Both phylogeny and function differentially affect craniodental morphology in extant and extinct rhinoceroses. This notion holds when two different comparative methods are applied. As expected, structures more thoroughly dedicated to mastication show the least covariation with phylogeny and the most covariation with the hypsodonty index. After applying the variation partitioning analysis, pure phylogeny's influence on shape variation decreases from skull to mandible to upper tooth row (occlusal view). In contrast, the

influence of pure HI increases from skull to mandible to upper tooth row. Yet, skull morphology shows a strong covariation with HI when the effect of the latter is estimated in interaction with phylogeny (phylogenetically structured functional variation), indicating that adaptation to different feeding styles occurs deep in the rhino tree rather than at the tips (that is, it applies above the species level). In the case of rhinos, such morphological changes include a different design of the posterior part of the skull, which is in fact known to change with feeding style. Pure size of the structures does not explain important portions of morphological variance.

The prediction that the structure least correlated with phylogeny and more correlated with pure HI (i.e. the upper tooth row) should be the least integrated with the other structures is confirmed by Escoufier's *RV* coefficient. This suggests that, whereas mandible and skull are constrained by phylogeny and (developmental) integration between each other, the upper tooth row is less influenced by this sort of covariation with other cranial structures, and therefore is the more free to evolve. This study confirms previous results obtained on carnivores (Dayan *et al.*, 2002), reaffirming that mammalian teeth are the most plastic cranial structure in evolutionary terms.

ACKNOWLEDGEMENTS

We are grateful to Mikael Fortelius and two anonymous reviewers for deep and insightful comments on the manuscript, which allowed us to produce a better picture of rhino craniodental evolution.

REFERENCES

Ackermann, R.R. and Cheverud, J.M. 2000. Phenotypic covariance structure in tamarins (genus *Saguinus*): a comparison of variation patterns using matrix correlation and common principal component analysis. *Am. J. Phys. Anthropol.*, **111**: 489–501.

Ackermann, R.R. and Cheverud, J.M. 2004a. Morphological integration in primate evolution. In *Phenotypic Integration: Studying the Ecology and Evolution of Complex Phenotypes* (M. Pigluicci and K. Preston, eds.), pp. 302–319. New York: Oxford University Press.

Ackermann, R.R. and Cheverud, J.M. 2004b. Detecting genetic drift versus selection in human evolution. *Proc. Natl. Acad. Sci. USA*, **101**: 17946–17951.

Adams, D.C. 2008. Phylogenetic meta-analysis. *Evolution*, **62**: 567–572.

Adams, D.C., Rohlf, F.J. and Slice, D.E. 2004. Geometric morphometrics: ten years of progress following the 'revolution'. *Ital. J. Zool.*, **71**: 5–16.

Agusti, J. and Anton, M. 2002. *Mammoths, Sabertooths and Hominids: 65 Million Years of Mammalian Evolution in Europe*. New York: Columbia University Press.

Anderson, M.J. 2003. *PCO: A FORTRAN Computer Program for Principal Coordinate Analysis*. Auckland: Department of Statistics, University of Auckland.

Antoine, P.O. 2002. Phylogénie et évolution des Elasmotheriina (Mammalia, Rhinocerotidae). *Mém. Mus. Nat. Hist. Nat. Paris*, **188**: 5–350.

Arnold, S.J. 1994. Investigating the origins of the performance advantage: adaptation, exaptation and lineage effects. In *Phylogenetics and Ecology* (P. Eggleton and R. Vane-Wright, eds.), pp. 123–168. London: Academic Press.

Arthur, W. 2001. Developmental drive: an important determinant of the direction of phenotypic evolution. *Evol. Develop.*, **3**: 271–278.

Atchley, W.R. 1993. Genetic and developmental aspects of variability in the mammalian mandible. In *The Skull, Vol. 1: Development* (J. Hanken and B.K. Hall, eds.), pp. 207–247. Chicago, IL: University of Chicago Press.

Atchley, W.R. and Hall, B.K. 1991. A model for development and evolution of complex morphological structures. *Biol. Rev. Cambr. Phil. Soc.*, **66**: 101–157.

Atchley, W.R., Nordheim, E.V., Gunsett, F.C. and Crump, P.L. 1982. Geometric and probabilistic aspects of statistical distance functions. *Syst. Zool.*, **31**: 445–460.

Badyaev, A.V. and Foresman, K.R. 2000. Extreme environmental change and evolution: stress-induced morphological variation is strongly concordant with patterns of evolutionary divergence in shrew mandibles. *Proc. R. Soc. Lond. B*, **267**: 371–377.

Badyaev, A.V. and Foresman, K.R. 2004. Evolution of morphological integration. I. Functional units channel stress-induced variation in shrew mandibles. *Am. Nat.*, **163**: 868–879.

Badyaev, A.V., Foresman, K.R. and Young, R.L. 2005. Evolution of morphological integration. II. Developmental accommodation of stress-induced variation in shrew mandibles. *Am. Nat.*, **166**: 382–395.

Bales, G.S. 1996. Skull evolution in the Rhinocerotidae (Mammalia, Perissodactyla): Cartesian transformations and functional interpretations. *J. Mammal. Evol.*, **3**: 261–279.

Bastir, M. and Rosas, A. 2005. The hierarchical nature of morphological integration and modularity in the human posterior face. *Am. J. Phys. Anthropol.*, **128**: 26–34.

Bastir, M. and Rosas, A. 2006. Correlated variation between the lateral basicranium and the face: a geometric morphometric study in different human groups. *Arch. Oral Biol.*, **51**: 814–824.

Blomberg, S.P., Garland, T., Jr. and Ives, A.R. 2003. Testing for phylogenetic signal in comparative data: behavioural traits are more labile. *Evolution*, **57**: 717–745.

Bookstein, F.L. 1986. Size and shape spaces for landmark data in two dimensions. *Stat. Sci.*, **1**: 181–242.

Bookstein, F.L. 1991. *Morphometric Tools for Landmark Data: Geometry and Biology*. Cambridge: Cambridge University Press.

Bookstein, F.L., Streissguth, A.P., Sampson, P.D., Connor, P.D. and Barr, H.H. 2002. Corpus callosum shape and neuropsychological deficits in adult males with heavy fetal alcohol exposure. *NeuroImage*, **15**: 233–251.

Borcard, D., Legendre, P., and Drapeau, P. 1992. Partialling out the spatial component of ecological variation. *Ecology*, **73**: 1045–1055.

Cerdeño, E. 1998. Diversity and evolutionary trends of the family Rhinocerotidae (Perissodactyla). *Palaeogeogr. Palaeoclimatol. Palaeoecol.*, **141**: 13–34.

Cheverud, J.M. 1982. Phenotypic, genetic, and environmental morphological integration in the cranium. *Evolution*, **36**: 499–516.

Cheverud, J.M. 1989. Evolution of morphological integration. In Trends in Vertebrate Morphology: Proceedings of the 2nd International Symposium on Vertebrate Morphology (H. Splechtna and H. Helge, eds.). *Fortschr. Zool.*, **35**: 196–197.

Cheverud, J.M. 1995. Morphological integration in the saddle-back tamarin (*Saguinus fuscicollis*) cranium. *Am. Nat.*, **145**: 63–89.

Cheverud, J.M. 1996. Developmental integration and the evolution of pleiotropy. *Am. Zool.*, **36**: 44–50.

Cheverud, J.M. 2004. Modular pleiotropic effects of quantitative trait loci on morphological traits. In *Modularity in Development and Evolution* (G. Schlosser & G.P. Wagner, eds.), pp. 132–153. Chicago, IL: University of Chicago Press.

Cheverud, J.M., Hartman, S.E., Richtsmeier, J.T. and Atchley, W.R. 1991. A quantitative genetic analysis of localized morphology in mandibles of inbred mice using finite element scaling analysis. *J. Craniofac. Genet. Dev. Biol.*, **11**: 122–137.

Cheverud, J.M., Leamy, L.J. and Routman, E.J. 1997. Pleiotropic effects of individual gene loci on mandibular morphology. *Evolution*, **51**: 2004–2014.

Cheverud, J.M., Ehrich, T.H., Vaughn, T.T., Koreishi, S.F., Linsey, R.B. and Pletscher, L.S. 2004. Pleiotropic effects on mandibular morphology II: Differential epistasis and genetic variation in morphological integration. *J. Exp. Zool. B: Molec. Develop. Evol.*, **302B**: 424–435.

Claude, J. 2008. *Morphometrics with R*. New York: Springer.

Clauss, M. and Hummel, J. 2005. The digestive performance of mammalian herbivores: why big may not be that much better. *Mammal. Rev.*, **35**: 174–187.

Clauss, M., Frey, R., Kiefer, B., Lechner-Doll, M., Loehlein, W., Polster, Cö. *et al.* 2003. The maximum attainable body size of herbivorous mammals: morphophysiological constraints on foregut, and adaptations of hindgut fermenters. *Oecologia*, **136**: 14–27.

Codron, D., Codron, J., Lee-Thorp, J.A., Sponheimer, D., de Ruiter, D., Sealy, J. *et al.* 2007. Diets of savanna ungulates from stable carbon isotope composition of faeces. *J. Zool.*, **273**: 21–29.

Cubo, J., Ponton, F., Laurin, M., De Margerie, E. and Castanet, J. 2005. Phylogenetic signal in bone microstructure of Sauropsids. *Syst. Biol.*, **54**: 562–574.

Cubo, J., Legendre, P., de Ricqlès, A., Montes, L., de Margerie, E., Castanet, J. *et al.* 2008. Phylogenetic, functional and structural components of variation in bone growth rate of amniotes. *Evol. Develop.*, **10**: 217–227.

Cumming, D.H.M., Du Toit, R.F. and Stuart, S.N. 1990. *African Elephants and Rhinos: Status Survey and Conservation Action Plan*. IUCN/SSC African Elephant and Rhino Specialist Group. Gland, Switzerland: IUCN.

Dayan, T., Wool, D. and Simberloff, D. 2002. Variation and covariation of skulls and teeth: modern carnivores and the interpretation of fossil mammals. *Paleobiology*, **28**: 508–526.

Demment, M.W. and Van Soest, P.J. 1985. A nutritional explanation for body-size patterns of ruminant and non-ruminant herbivores. *Am. Nat.*, **125**: 1–641.

Desdevises, Y., Legendre, P., Azouzi, L. and Morand, S. 2003. Quantifying phylogenetically structured environmental variation. *Evolution*, **57**: 2647–2652.

Dierenfeld, E. 1995. Rhinoceros nutrition: an overview with special reference to browsers. *Verh. Ber. Erkrg. Zootiere*, **37**: 7–14.

Diniz-Filho, J.A.F., Sant'ana, C.E.R. and Bini, L.M. 1998. An eigenvector method for estimating phylogenetic inertia. *Evolution*, **52**: 1247–1262.

Drake, A.G. and Klingenberg, C.P. 2010. Large-scale diversification of skull shape in domestic dogs: disparity and modularity. *Am. Nat.*, **175**: 289–301.

Ehrich, T.H., Vaughn, T.T., Koreishi, S.F., Linsey, R.B., Pletscher, L.S. and Cheverud, J.M., 2003. Pleiotropic effects on mandibular morphology II. Developmental morphological integration and differential dominance. *J. Exp. Zool. B: Molec. Develop. Evol.*, **296B**: 58–79.

Emslie, R. and Brooks, M. 1999. *African Rhino: Status Survey and Conservation Action Plan*. Gland, Switzerland: IUCN.

Escoufier, Y. 1973. Le traitement des variables vectorielles. *Biometrics*, **29**: 751–760.

Felsenstein, J. 1985. Phylogenies and the comparative method. *Am. Nat.*, **125**: 1–15.

Feranec, R.S. 2007. Ecological generalization during adaptive radiation: evidence from Neogene mammals. *Evol. Ecol.*, **9**: 555–577.

Fortelius, M. 1981. Functional aspects of occlusal cheek-tooth morphology in hypsodont, non-ruminant ungulates. In *International Symposium on Concept and Method in Paleontology: Contributed Papers* (J. Martinell, ed.), pp. 153–162. Barcelona: University of Barcelona.

Fortelius, M. 1982. Ecological aspects of dental functional morphology in the Plio-Pleistocene rhinoceroses of Europe. In *Teeth: Form, Function and Evolution* (B. Kurten, ed.), pp. 163–181. New York: Columbia University Press.

Fortelius, M. and Solounias, N. 2000. Functional characterization of ungulate molars using the abrasion–attrition wear gradient: a new method for reconstructing paleodiets. *Am. Mus. Nov.*, **3301**: 1–36.

Fortelius, M., Mazza, P. and Sala, B. 1993. *Stephanorhinus* (Mammalia, Rhinocerotidae) of the western European Pleistocene, with a special revision of *Stephanorhinus etruscus* (Falconer, 1868). *Pal. Ital.*, **80**: 63–155.

Frontier, S. 1976. Étude de la décroissance des valeurs propres dans une analyse en composantes principales: comparaison avec le modèle du bâton brisé. *J. Exp. Mar. Biol. Ecol.*, **25**: 67–75.

Garland, T., Jr. 1992. Rate tests for phenotypic evolution using phylogenetically independent contrasts. *Am. Nat.*, **140**: 509–519.

Garland, T., Jr., Harvey, P.H. and Ives, A.R. 1992. Procedures for the analysis of comparative data using phylogenetically independent contrasts. *Syst. Biol.*, **41**: 18–32.

Garland, T., Jr., Dickerman, A.W., Janis, C.M. and Jones, J.A. 1993. Phylogenetic analysis of covariance by computer simulation. *Syst. Biol.*, **42**: 265–292.

Garland, T., Jr., Bennett, A.F. and Rezende, E.L. 2005. Phylogenetic approaches in comparative physiology. *J. Exp. Biol.*, **208**: 3015–3035.

Geraads, D. 2005. Pliocene Rhinocerotidae (Mammalia) from Hadar e Dikika (Lower Awash, Ethiopia) and a revision of the origin of modern African rhinos. *J. Vert. Paleontol.*, **25**: 451–461.

Giaourtsakis, I., Theodorou, G., Roussiakis, S., Athanassiou, A. and Iliopoulos, G. 2006. Late Miocene horned rhinoceroses (Rhinocerotinae, Mammalia) from Kerassia (Euboea, Greece). *N. Jb. Geol. Pal. Abh.*, **239**: 367–398.

Gordon, I.J. and Illius, A.W. 1988. Incisor arcade structure and diet selection in ruminants. *Funct. Ecol.*, **2**: 15–22.

Goswami, A. 2006. Cranial modularity shifts during mammalian evolution. *Am. Nat.*, **168**: 270–280.

Goswami, A. and Polly, P.D. 2010. The influence of modularity on cranial morphological disparity in Carnivora and Primates (Mammalia). *PLoS One*, **5**(3): e9517, 1–8.

Goswami, A. and Prochel, J. 2007. Ontogenetic morphology and cranial allometry of the common European mole (*Talpa europaea*). *J. Mammal.*, **88**: 667–677.

Gould, S.J. 2002. *The Structure of Evolutionary Theory*. Cambridge, MA: Belknap Press of Harvard University Press.

Gould, S.J. and Lewontin, R.C. 1979. The spandrels of San Marco and the Panglossian paradigm: a critique of the adaptationist programme. *Proc. R. Soc. Lond. B*, **205**: 581–598.

Gould, S.J. and Vrba, E.S. 1982. Exaptation – a missing term in the science of form. *Paleobiology*, **8**: 4–15.

Groves, C.P. and Kurt, F. 1972. *Dicerorhinus sumatrensis. Mammal. Species*, **21**: 1–6.

Guérin, C. 1980. Les rhinocéros (Mammalia, Perissodactyla) du Miocène terminal au Pléistocène supérieur en Europe occidentale. Comparaison avec les espèces actuelles. *Doc. Lab. Géol. Lyon*, **79**: fasc. 1, 2, 3, 1185 pp.

Hallgrímsson, B., Willmore, K. and Hall, B. 2002. Canalization, developmental stability, and morphological integration in primate limbs. *Yearbook Phys. Anthropol.*, **45**: 131–158.

Harmon, L., Weir, J., Brock, C., Glor, R., Challenger, W. and Hunt, G. 2009. *GEIGER: Analysis of Evolutionary Diversification. R package version 1.3–1* (http://CRAN.R-project.org/package=Geiger).

Harvey, P.H. and Pagel, M.D. 1991. *The Comparative Method in Evolutionary Biology*. Oxford: Oxford University Press.

Heissig, K. 1989. The Rhinocerotidae. In *The Evolution of Perissodactyls* (D.R. Prothero and R.M. Schoch, eds.), pp. 399–417. New York: Oxford University Press.

Janis, C.M. 1976. The evolutionary strategy of the Equidae and the origin of rumen and cecal digestion. *Evolution*, **30**: 757–774.

Janis, C.M. 1995. Correlations between craniodental morphology and feeding behaviour in ungulates: reciprocal illumination between living and fossil taxa. In *Functional Morphology in Vertebrate Paleontology* (J.J. Thomason, ed.), pp. 76–98. Cambridge: Cambridge University Press.

Janis, C.M. 2008. An evolutionary history of browsing and grazing ungulates. In *The Ecology of Browsing and Grazing* (I.J. Gordon and H.H.T. Prins, eds.), pp. 21–45. Berlin: Springer.

Josse, S., Moreau, T. and Laurin, M. 2006. *Stratigraphic Tools for Mesquite* (http://mesquiteproject.org/packages/stratigraphicTools).

Kahlke, R.D. and Kaiser, T.M. in press. Generalism as a subsistence strategy: advantages and limitations of the highly flexible feeding traits of Pleistocene *Stephanorhinus hundsheimensis* (Rhinoceritidae, Mammalia). *Quat. Sci. Rev.*

Kahlke, R.D. and Lacombat, F. 2008. The earliest immigration of woolly rhinoceros (*Coelodonta tologoijensis*, Rhinocerotidae, Mammalia) into Europe and its adaptive evolution in Palaearctic cold stage mammal faunas. *Quat. Sci. Rev.*, **27**: 1951–1961.

Klingenberg, C.P. 2005. Developmental constraints, modules and evolvability. In *Variation: A Central Concept in Biology* (B. Hallgrímsson and B.K. Hall, eds.), pp. 219–247. Burlington, MA: Elsevier.

Klingenberg, C.P. 2009. Morphometric integration and modularity in configurations of landmarks: tools for evaluating *a-priori* hypotheses. *Evol. Develop.*, **11**: 405–421.

Klingenberg, C.P. 2011. MorphoJ: an integrated software package for geometric morphometrics. *Molec. Ecol. Res*. (DOI: 10.1111/j.1755-0998.2010.02924.x).

Klingenberg, C.P. and Leamy, L.J. 2001. Quantitative genetics of geometric shape in the mouse mandible. *Evolution*, **55**: 2342–2352.

Klingenberg, C.P., Leamy, L.J., Routman, E.J. and Cheverud, J.M. 2001. Genetic architecture of mandible shape in mice: effects of quantitative trait loci analyzed by geometric morphometrics. *Genetics*, **157**: 785–802.

Klingenberg, C.P., Barluenga, M. and Meyer, A. 2003. Body shape variation in cichlid fishes of the *Amphilophus citrinellus* species complex. *Biol. J. Linn. Soc.*, **80**: 397–408.

Klingenberg, C.P., Leamy, L.J. and Cheverud, J.M. 2004. Integration and modularity of quantitative trait locus effects on geometric shape in the mouse mandible. *Genetics*, **166**: 1909–1921.

Lacombat, F. 2003. *Étude des rhinocéroses du Pléistocène de l'Europe méditerranéenne et du Massif Central. Paléontologie, phylogénie et biostratigraphie*. Unpublished DPhil thesis. Paris : Museum National d'Histoire Naturelle.

Laurie, W.A. 1982. Behavioural ecology of the greater one-horned rhinoceros (*Rhinoceros unicornis*). *J. Zool.*, **196**: 307–341.

Laurie, W.A., Lang, E.M. and Groves, C.P. 1983. *Rhinoceros unicornis. Mammal. Species*, **211**: 1–6.

Lavin, S.R., Karasov, W.H., Ives, A.R., Middleton, K.M. and Garland, T., Jr. 2008. Morphometrics of the avian small intestine compared with that of nonflying mammals: a phylogenetic approach. *Physiol. Biochem. Zool.*, **81**: 526–550.

Leamy, L.J., Routman, E.J. and Cheverud, J.M. 1999. Quantitative trait loci for early and late developing skull characters in mice: a test of the genetic independence model of morphological integration. *Am. Nat.*, **153**: 201–214.

Leamy, L.J., Routman, E.J. and Cheverud, J.M. 2002. An epistatic genetic basis for fluctuating asymmetry of mandible size in mice. *Evolution*, **56**: 642–653.

Lieberman, D.E., Ross, C.F. and Ravosa, M.J. 2000. The primate cranial base: ontogeny, function, and integration. *Yearbook Phys. Anthropol.*, **43**: 117–169.

Loose, H. 1975. Pleistocene Rhinocerotidae of W. Europe with reference to the recent two-horned species of Africa and S.E. Asia. *Scr. Geol.*, **33**: 1–59.

Louys, J., Curnoe, D. and Tong, H. 2007. Characteristics of Pleistocene megafauna extinctions in Southeast Asia. *Palaeogeogr. Palaeoclimatol. Palaeoecol.*, **243**: 152–173.

Maddison, W.P. and Maddison, D.R. 2007. *Mesquite: A Modular System for Evolutionary Analysis*, Version 2.01 (http://mesquiteproject.org).

Marcus, L.F., Hingst-Zaher, E. and Zaher, H. 2000. Application of landmarks morphometrics to skull representing the orders of living mammals. *Hystrix*, **11**: 27–47.

Márquez, E.J. 2008. A statistical framework for testing modularity in multidimensional data. *Evolution*, **62**: 2688–2708.

Marroig, G. and Cheverud, J.M. 2001. A comparison of phenotypic variation and covariation patterns and the role of phylogeny, ecology, and ontogeny during cranial evolution of New World monkeys. *Evolution*, **55**: 2576–2600.

Marroig, G., De Vivo, M. and Cheverud, J.M. 2004. Cranial evolution in sakis (Pithecia, Platyrrhini) II: Evolutionary processes and morphological integration. *J. Evol. Biol.*, **17**: 144–155.

Martins, E.P., Diniz-Filho, J.A.F. and Housworth, E.A. 2002. Adaptive constraints and the phylogenetic comparative method: a computer simulation test. *Evolution*, **56**: 1–13.

Maynard Smith, J., Burian, R., Kaufman, S., Alberch, P. and Campbell, J. 1985. Developmental constraints and evolution. *Quart. Rev. Biol.*, **60**: 265–287.

Mazza, P. and Azzaroli, A. 1993. Ethological inferences on Pleistocene rhinoceroses of Europe. *Rend. Fis. Accad. Lincei*, **4**: 127–137.

McCullagh, P. 1980. Regression models for ordinal data. *J. R. Stat. Soc. Lond. B (Methodological)*, **42**: 109–142.

Meloro, C., Raia, P., Piras, P., Barbera, C. and O'Higgins, P. 2008. The shape of the mandibular corpus in large fissiped carnivores: allometry, function and phylogeny. *Zool. J. Linn. Soc.*, **154**: 832–845.

Mendoza, M. and Palmqvist, P. 2008. Hypsodonty in ungulates: an adaptation for grass consumption or for foraging in open habitat? *J. Zool.*, **274**: 134–142.

Mendoza, M., Janis, C.M. and Palmqvist, P. 2002. Characterizing complex craniodental patterns related to feeding behaviour in ungulates: a multivariate approach. *J. Zool.*, **258**: 223–246.

Mullin, S.K. and Taylor, P.J. 2002. The effects of parallax on geometric morphometric data. *Comp. Biol. Med.*, **32**: 455–464.

Nanda, A.C. 2002. Upper Siwalik mammalian faunas of India and associated events. *J. Asian Earth Sci.*, **21**: 47–58.

Nowak, R.M. 1991. *Walker's Mammals of the World*. Baltimore, MD: Johns Hopkins University Press.

Ohtani, K. 2000. Bootstrapping R^2 and adjusted R^2 in regression analysis. *Econ. Model.*, **17**: 473–483.

Oksanen, J., Kindt, R., Legendre, P., O'Hara, B., Simpson, G.L., Solymos, P. *et al.* 2008. *Vegan: Community Ecology Package*. R Package version 1.15–1 (http:// cran.r-project.org/, http:// vegan.r-forge.r-project.org/).

Orlando, L., Leonard, J.A., Thenot, A., Laudet, V., Guérin, C. and Hänni, C. 2003. Ancient DNA analysis reveals woolly rhino evolutionary relationships. *Molec. Phylogenet. Evol.*, **28**: 485–499.

Owen-Smith, R.N. 1988. *Megaherbivores: The Influence of Very Large Body Size on Ecology*. Cambridge: Cambridge University Press.

Peres-Neto, P.R., Legendre, P., Dray, S. and Borcard, D. 2006. Variation partitioning of species data matrices: estimation and comparison of fractions. *Ecology*, **87**: 2614–2625.

Perez, S.I., Bernal, V. and Gonzalez, P.N. 2006. Differences between sliding semi-landmark methods in geometric morphometrics, with an application to human craniofacial and dental variation. *J. Anat.*, **208**: 769–784.

Perez-Barberia, F.J. and Gordon, I.J. 1999. The functional relationship between feeding type and jaw and cranial morphology in ungulates. *Oecologia*, **118**: 157–165.

Perez-Barberia, F.J. and Gordon, I.J. 2001. Relationships between oral morphology and feeding style in the Ungulata: a phylogenetically controlled evaluation. *Proc. R. Soc. Lond. B*, **268**: 1023–1032.

Piras, P., Colangelo, P., Adams, D.C., Buscalioni, A., Cubo, J., Kotsakis, T. *et al.* 2010. The *Gavialis–Tomistoma* debate: the contribution of skull ontogenetic allometry and growth trajectories to the study of crocodylian relationships. *Evol. Develop.*, **12**: 568–579.

Polly, P.D. 2005. Development and phenotypic correlations: the evolution of tooth shape in *Sorex araneus*. *Evol. Develop.*, **7**: 29–41.

Pratiknyo, H. 1991. The diet of the Javan rhino. *Voice Nat.*, **93**: 12–13.

Prithiviraj, F., Polet, G., Foead, N., Ng, L., Pastorini, J. and Melnick, D.J. 2006. Genetic diversity, phylogeny and conservation of the Javan rhinoceros (*Rhinoceros sondaicus*). *Conserv. Genet.*, **7**: 439–448.

Raia, P., Carotenuto, F., Meloro, C., Piras, P. and Pushkina, D. 2010. The shape of contention: adaptation, history and contingency in ungulate mandibles. *Evolution*, **64**: 1489–1503.

Ramette, A. and Tiedje, J. 2007. Multiscale responses of microbial life to spatial distance and environmental heterogeneity in a patchy ecosystem. *Proc. Natl. Acad. Sci. USA*, **104**: 2761–2766.

R Development Core Team (2010). *R: A Language and Environment for Statistical Computing*. Vienna, Austria: R Foundation for Statistical Computing (URL: http://www.R-project.org).

Rohlf, F.J. 2001. Comparative methods for the analysis of continuous variables: geometric interpretations. *Evolution*, **55**: 2143–2160.

Rohlf, F.J. 2005. *tpsDig, Digitize Landmarks and Outlines*. Version 2.05. Department of Ecology and Evolution, State University of New York at Stony Brook.

Rohlf, F.J. 2006. A comment on phylogenetic corrections. *Evolution*, **60**: 1509–1515.

Schwenk, K. 1995. A utilitarian approach to evolutionary constraint. *Zoology*, **98**: 251–262.

Shrader, A.M., Owen-Smith, N. and Ogutu, J.O. 2006. How a mega-grazer copes with the dry season: food and nutrient intake rates by white rhinoceros in the wild. *Funct. Ecol.*, **20**: 376–384.

Solounias, N., Teaford, M. and Walker, A. 1988. Interpreting the diet of extinct ruminants: the case of a non-browsing giraffid. *Paleobiology*, **14**: 287–300.

Solounias, N., Moelleken, S.M.C. and Plavcan, J.M. 1995. Predicting the diet of extinct bovids using masseteric morphology. *J. Vert. Paleontol.*, **15**: 795–805.

Spencer, LM. 1995. Morphological correlates of dietary resource partitioning in the African Bovidae. *J. Mammal.*, **76**: 448–471.

Sponheimer, M., Lee-Thorp, J.A., DeRuiter, D.J., Smith, J.M., van der Merwe, N.J., Reed, K. *et al.* 2003. Diets of southern African bovidae: stable isotope evidence. *J. Mammal.*, **84**: 471–479.

Strait, D.S. 2001. Integration, phylogeny, and the hominid cranial base. *Am. J. Phys. Anthropol.*, **114**: 273–297.

Strömberg, C.A.E. 2006. The evolution of the hypsodonty in equids: testing a hypothesis of adaptation. *Paleobiology*, **32**: 236–258.

Tong, H. 2001. Rhinocerotids in China, systematics and material analysis. *Geobios*, **34**: 585–591.

Tougard, C., Delefosse, T., Hänni, C. and Montgelard, C. 2001. Phylogenetic relationships of the five extant rhinoceros species (Rhinocerotidae, Perissodactyla) based on mitochondrial cytochrome b and 12S rRNA genes. *Molec. Phylogenet. Evol.*, **19**: 34–44.

Wagner, G.P. and Altenberg, L. 1996. Complex adaptations and the evolution of evolvability. *Evolution*, **50**: 967–976.

Westoby, M., Leishmann, M.R. and Lord, J.M. 1995. On misinterpreting the 'phylogenetic correction'. *J. Ecol.*, **83**: 531–534.

Williams, S.H. and Kay, R.F. 2001. A comparative test for adaptive explanations for hypsodonty in ungulates and rodents. *J. Mammal. Evol.*, **8**: 207–229.

Young, N.M. and Hallgrímsson, B. 2005. Serial homology and the evolution of mammalian limb covariation structure. *Evolution*, **59**: 2691–2704.

Zelditch, M.L. 1988. Developmental and functional constraints on phenotypic covariation during growth and evolution. *Dissert. Abstr. Intern. B Sci. Engineer.*, **48**: 1912–1913.

Zelditch, M.L. and Carmichael, A.C. 1989a. Ontogenetic variation in patterns of developmental and functional integration in skulls of *Sigmodon fulviventer*. *Evolution*, **43**: 814–824.

Zelditch, M.L. and Carmichael, A.C. 1989b. Growth and intensity of integration through postnatal growth in the skull of *Sigmodon fulviventer*. *J. Mammal.*, **70**: 477–484.

Zelditch, M.L. and Moscarella, R.A. 2004. Form, function, and life history: Spatial and temporal dynamics of integration. In *Phenotypic Integration: Studying the Ecology and Evolution of Complex Phenotypes* (M. Pigluicci and K. Preston, eds.), pp. 274–301. New York: Oxford University Press.

Zelditch, M.L., Wood, A.R. and Swiderski, D.L. 2009. Building developmental integration into functional systems: function-induced integration of mandibular shape. *Evol. Biol. (New York)*, **36**: 71–87.

Zeuner, F.E. 1934. Die Beziehungen zwischen Schädelform und Lebensweise bei den rezenten und fossilen Nashörnern. *Ber. Naturf. Ges. Freiburg i. B*, **34**: 31–80.